

Content Adaptive Morphological Filtering: Thin Objects

Hugues Talbot¹ and Michael H.F. Wilkinson²

¹ Laboratoire d'Informatique Gaspard Monge, Université Paris-Est
ESIEE, France

² Johann Bernoulli Institute, University of Groningen, The
Netherlands

Vessel connectivity

- Connectivity is crucial for vessel identification and classification (i.e. vein, artery). We need this information for instance for pre-op planning.
- However noise causes disconnections and denoising typically is not enough to reconnect.
- So we need to be more "forceful".



Reconnection must be spatially variant

- A natural idea for a morphologist might be to use openings or closings for reconnecting disconnected vessels.
- However, using standard morphology with a spatially invariant structuring element will not work



(a) Noisy vessels



(b) SI closing



(c) SV closing



SV and adjunction

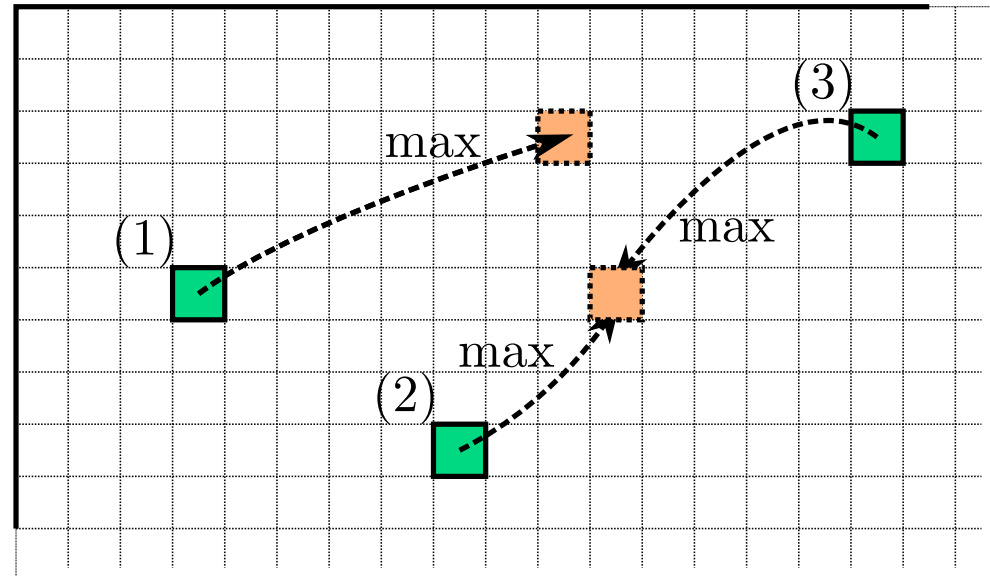
- Defining a SV erosion or dilation is *easy*
- Defining their SV adjunct dilation or erosion (resp.) is *not so easy*

$$\forall x \in \mathcal{L}, \forall y \in \mathcal{M}, \delta(x) \leq y \iff x \leq \varepsilon(y)$$

- We still have $\delta_B(I) = \bigvee_{p \in B} I_p$ adjunct to $\varepsilon_B(I) = \bigwedge_{p \in \check{B}} I_p$
- However, we need to consider the full definition of the transpose of a SE

$$\check{B}(x) = \{y \mid x \in B(y)\}, \quad (1)$$

- In the SI case, $\check{B}(x) = -B(x)$, but not in the SV case.
- It is possible to *compute it* but inefficient in the SVMM case.
- Fortunately we have an alternative.

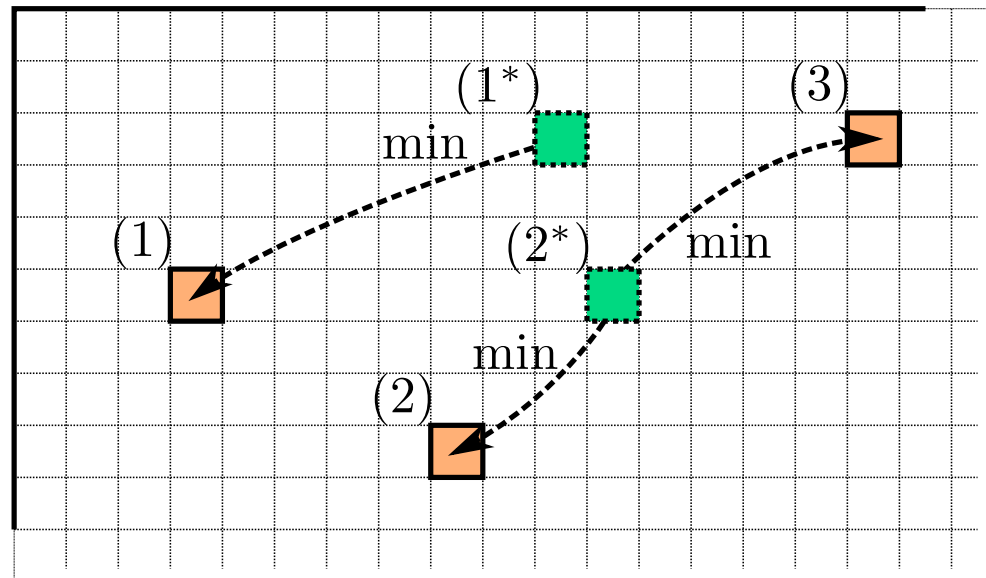
 δ_B 

Spatially variant dilation

This is easy to compute.

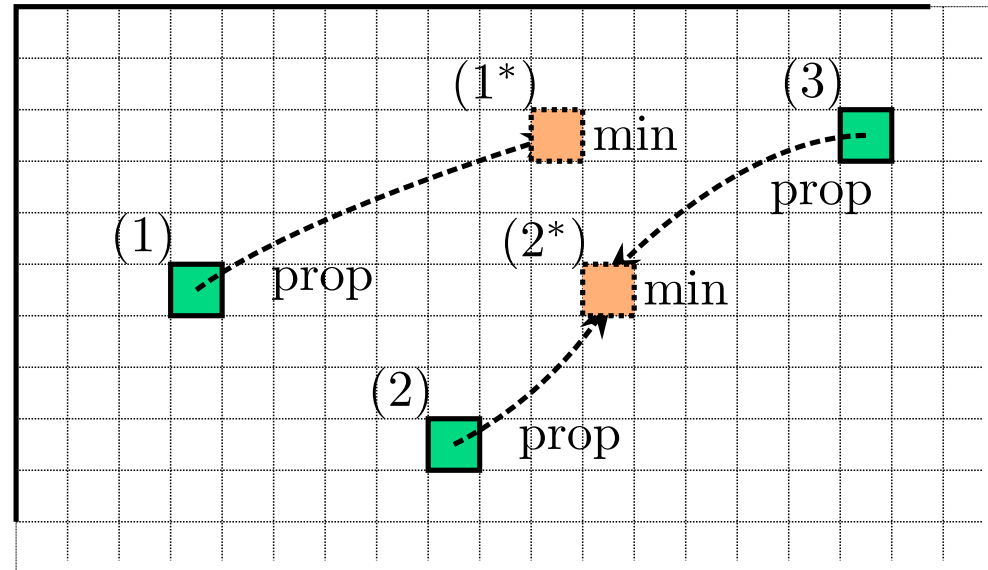


\mathcal{E}_B



Spatially variant adjunct erosion with computed SE

This can be expensive to compute.

 ε_B^* 

Spatially variant adjunct erosion alternative definition

This operator is equivalent to the adjunct erosion, and is as efficient to compute as the initial dilation.



- Let (E, Γ) be a graph with vertices E and oriented edges Γ (a.k.a arcs). if x is a vertex, we denote $\Gamma(x)$ its successors in the graph.
- Let $S \in E$ be a subset of E , then

$$\varepsilon_\Gamma(S) = \{\Gamma(x), x \in S\} \quad (2)$$

- Let ψ be an operator on (E, Γ) , then we define the dual of ψ for any subset S of E , as $\psi^*(S) = \overline{\psi(\overline{S})}$, where \overline{S} is the set complement of S .
- Then, the adjunct of ε_Γ is:

$$\delta_\Gamma = \varepsilon_{\Gamma^{-1}}^*, \quad (3)$$

where (E, Γ^{-1}) is the symmetric graph of (E, Γ) , i.e. where all the edge orientations have been reversed.



- This extends the standard erosions and dilations, which correspond to Γ being a regular, reflexive, symmetric graph.
- E.g., with E arranged in a regular square grid, Γ the 4-connected reflexive connectivity, this defines the standard erosion / dilation pair with the 4-connected neighborhood.
- Arbitrary structuring elements are defined by the equivalent graph connectivity.
- Openings and closings are defined as usual:

$$\gamma_\Gamma = \delta_\Gamma \circ \varepsilon_\Gamma \quad (\text{opening}) \tag{4}$$

$$\phi_\Gamma = \varepsilon_\Gamma \circ \delta_\Gamma \quad (\text{closing}) \tag{5}$$

- Grey-level operators are formally defined by threshold decomposition, but implemented efficiently with a max or min operator.

Filtering pipeline

- Filter the image to eliminate noise with an efficient NLM implementation (MPI + GPU , 5s for a $200 \times 200 \times 200$ image).
- Detect tubular objects using Frangi's vesselness
- Reconnect vessels with a spatially variant closing.

No problem in theory, however to reconnect vessels we require a dense direction field.

Dense direction field

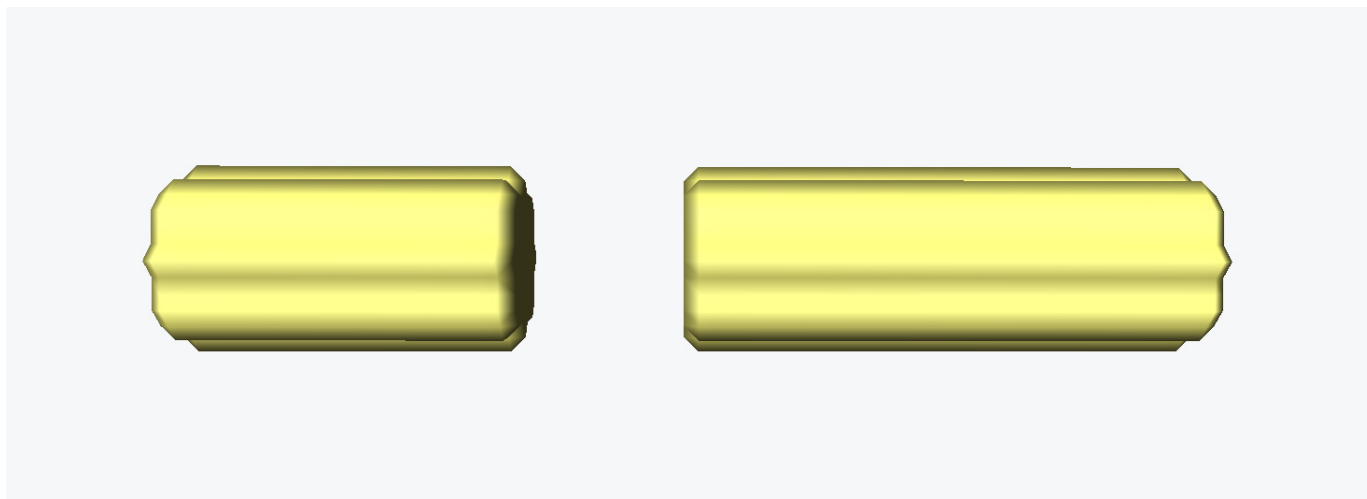
We need to:

- Estimate vessel directions from the Hessian eigenvectors
- Robustify these directions by sampling them near the center of the vessels
- Dilate the direction field
- Perform the SV closing with a segment oriented along these directions



university of
groningen

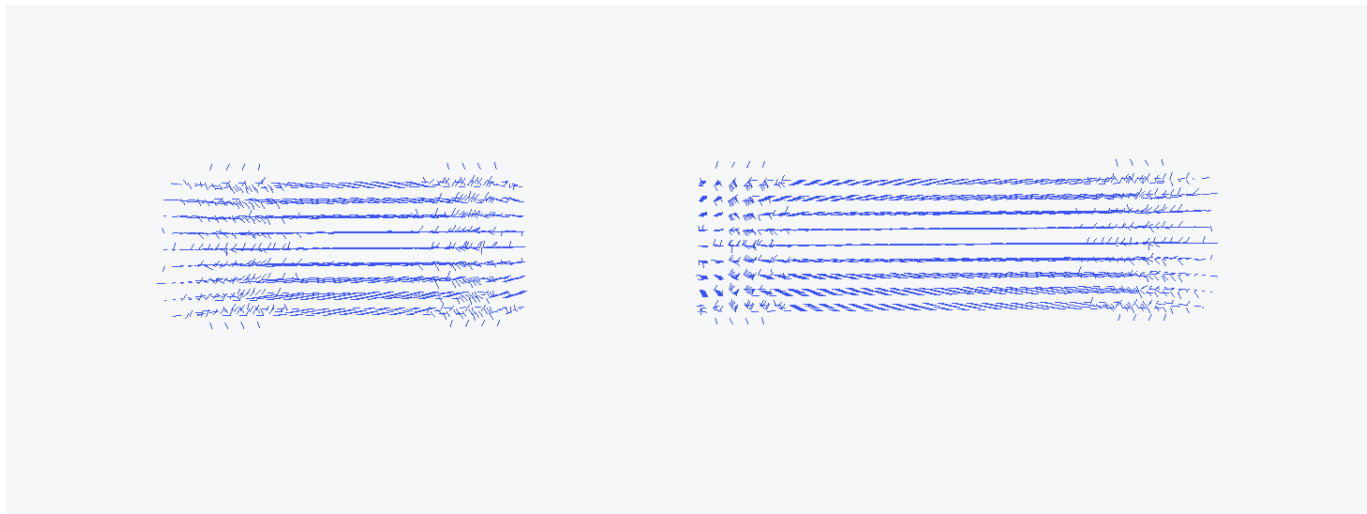
SV closing illustration





university of
groningen

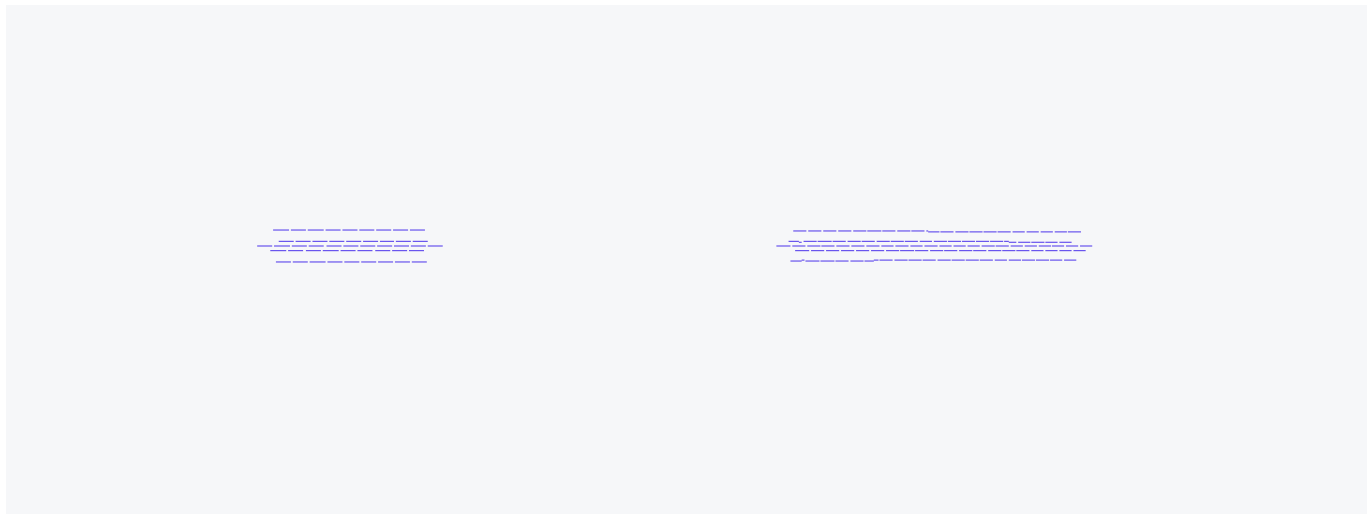
SV closing illustration





university of
groningen

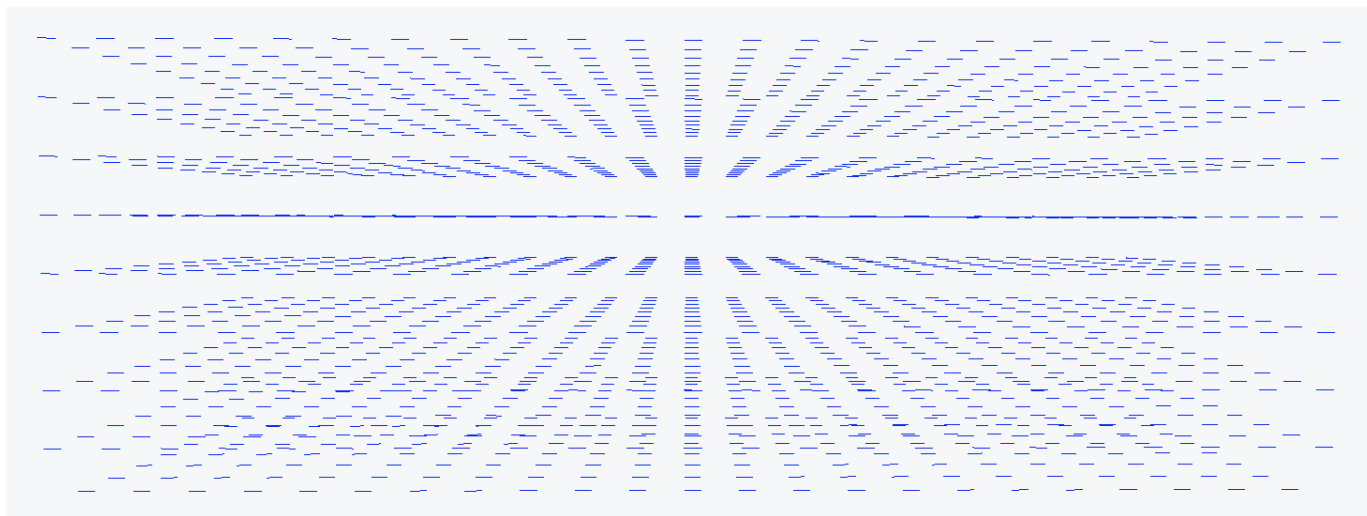
SV closing illustration





university of
groningen

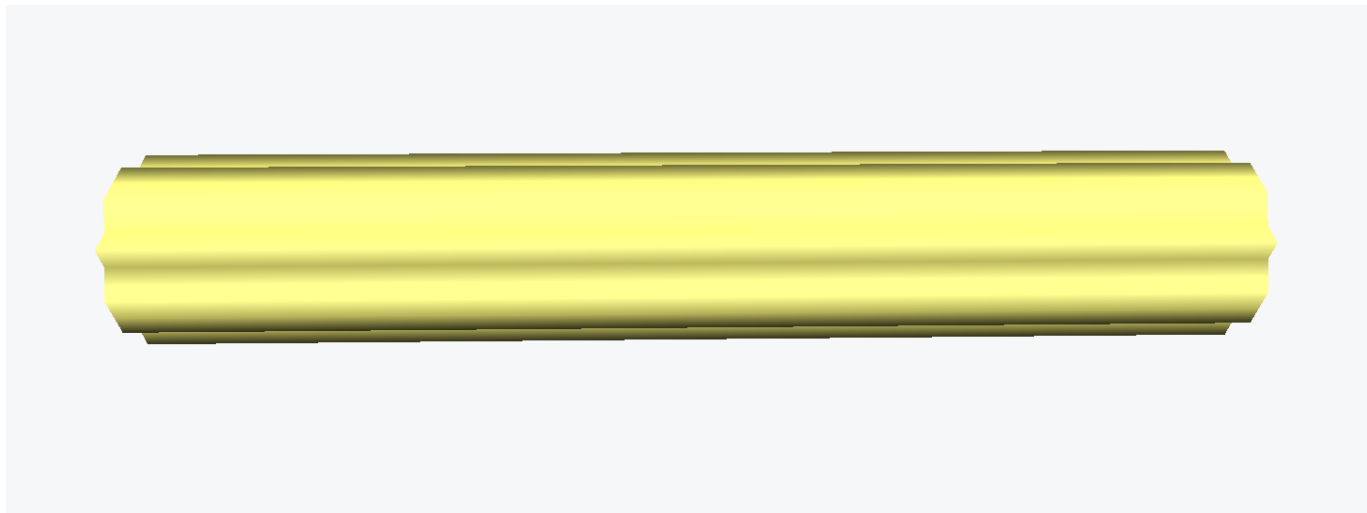
SV closing illustration

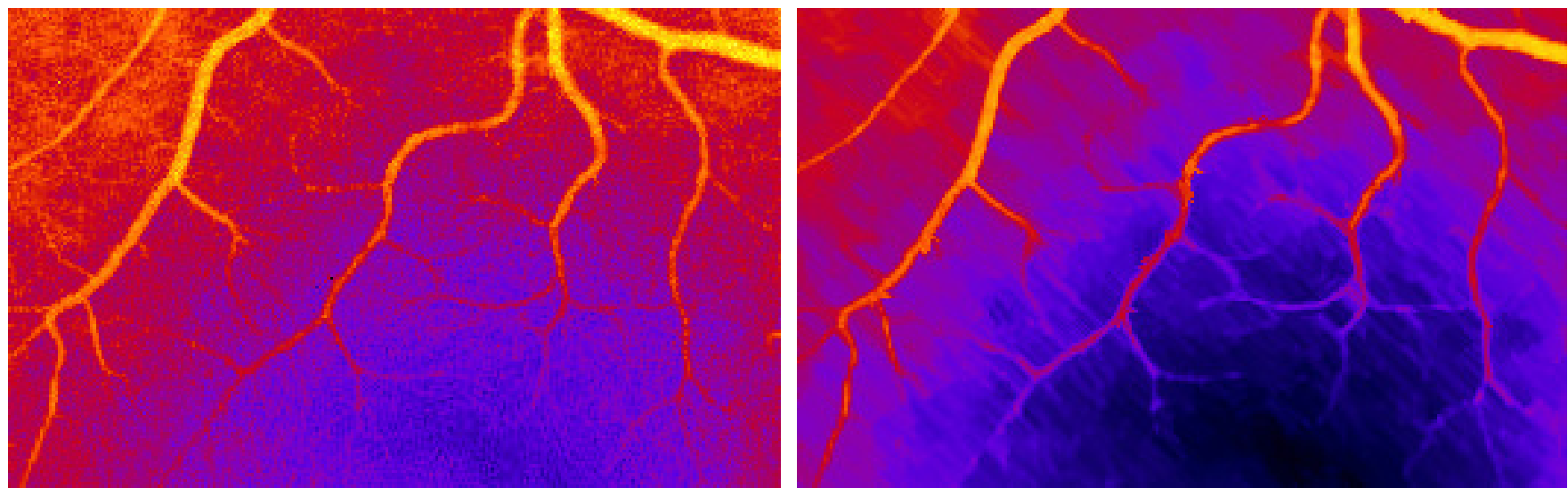




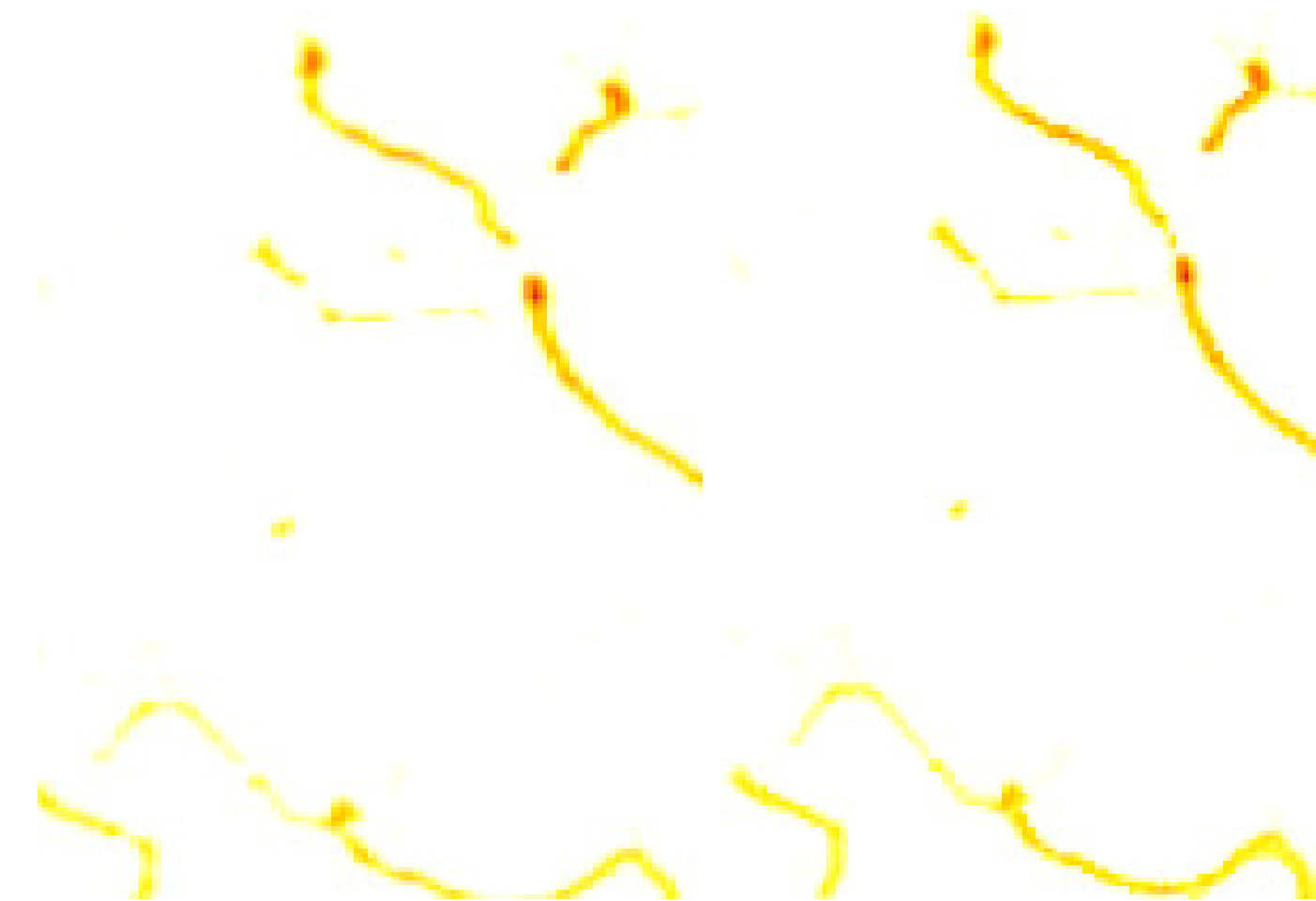
university of
groningen

SV closing illustration

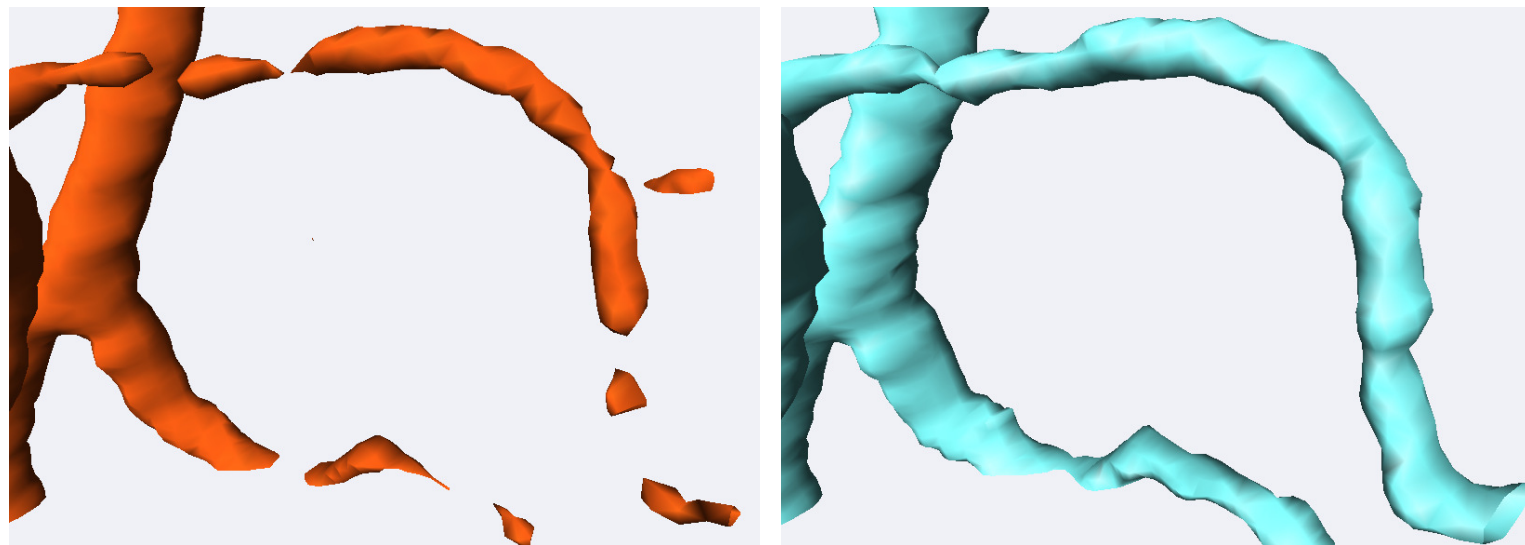




Eye fundus filtering



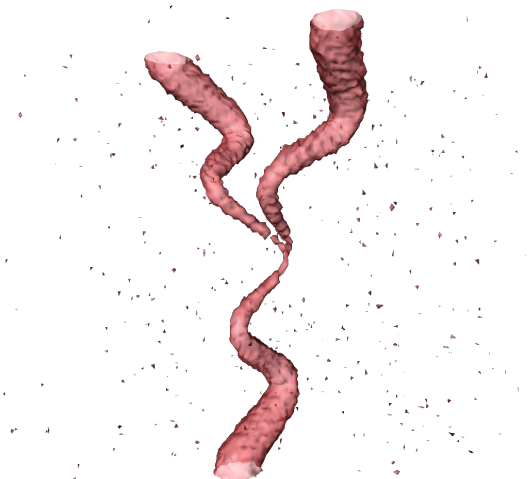
Neurite filtering

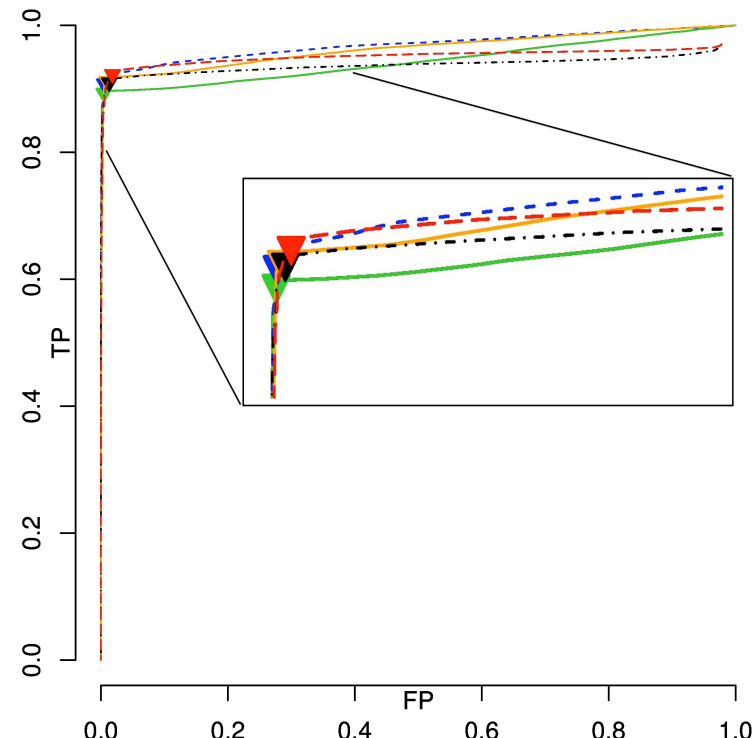
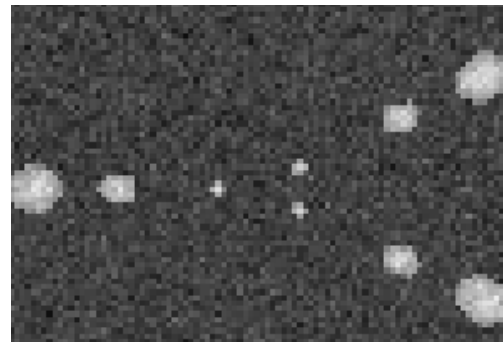


3D image of vessels in the brain

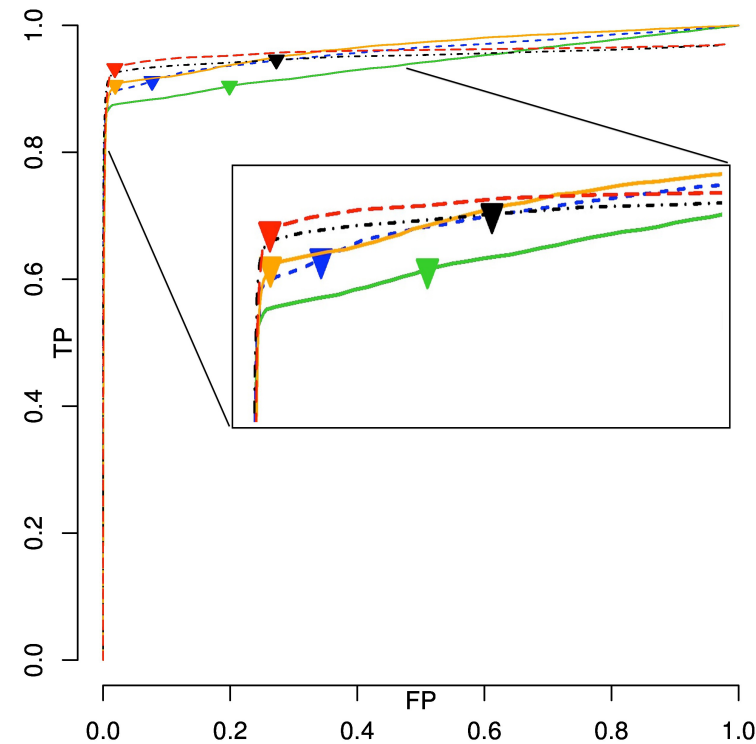
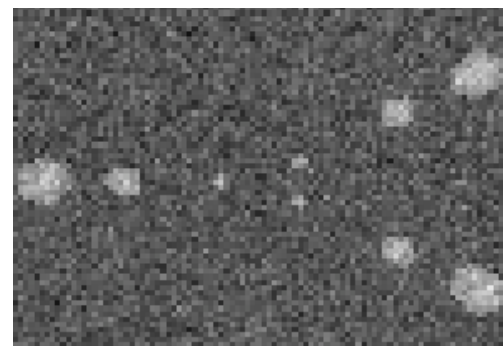
Description and origin

- We use a phantom from [8], which is a $100 \times 100 \times 100$ image used in a MICCAI workshop.
- It is tortuous and vessel-like
- grey-level with a parabolic intensity from 200 at the center to 150 at the edges. The background is 100, consistent e.g. with TOF MRA.
- In the following ROC analyses, the triangle indicates best fully-connected result.

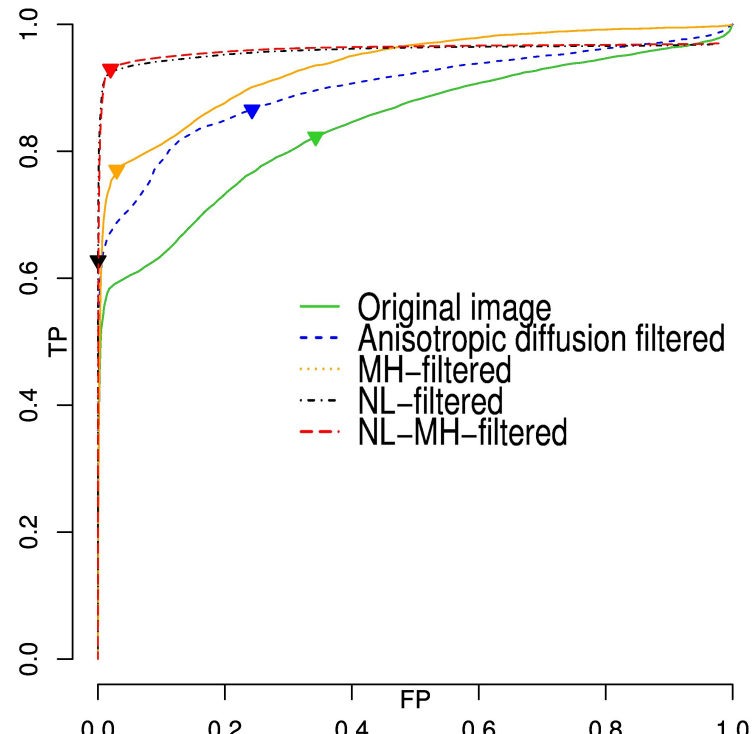
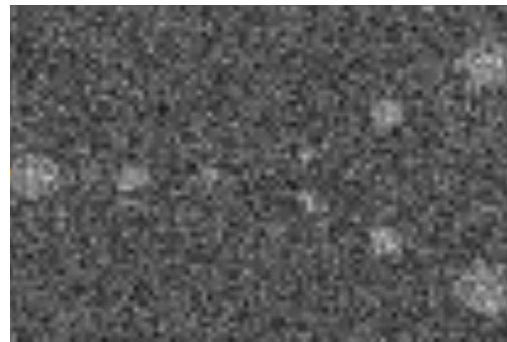




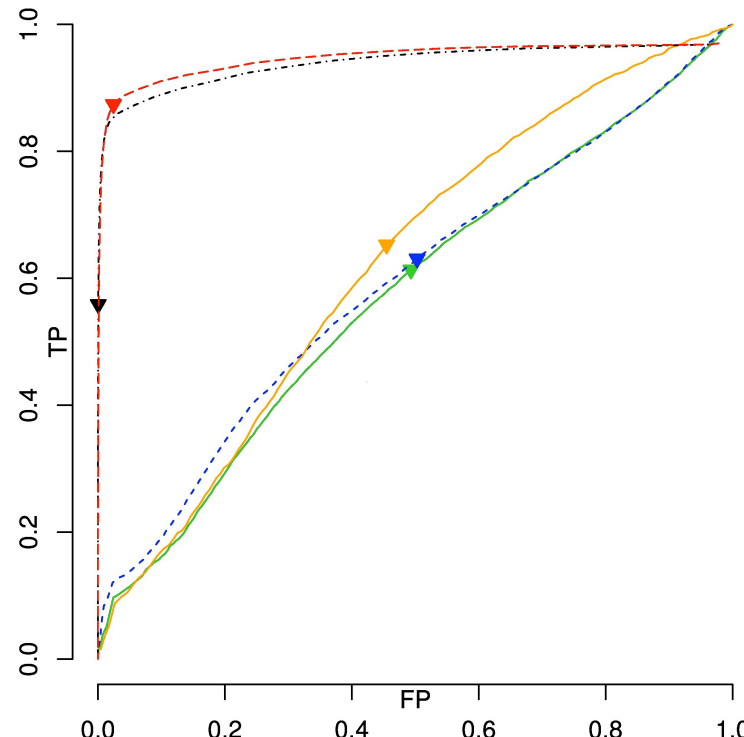
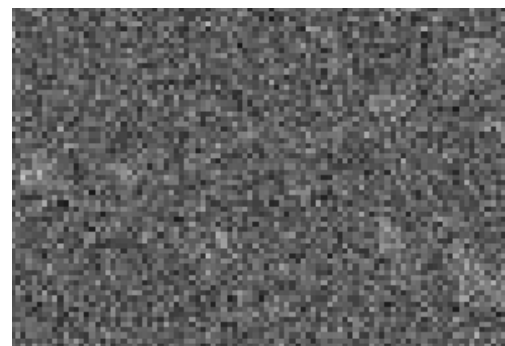
Level of noise standard deviation $\sigma = 10$



Level of noise standard deviation $\sigma = 20$



Level of noise standard deviation $\sigma = 40$



Level of noise standard deviation $\sigma = 80$

Notice that the filtered phantom remains connected even at very high noise levels.



Remarks

- Noise reduction achieved with non-local approaches, orientation measured by vesselness, reconnection achieved by Spatially Variant morphology.
- Combining noise reduction techniques with morphology allows us to achieve extremely robust results for thin object detection

Publications This work is described in greater detail in [25], as well as [26, 22, 23, 24, 6, 7, 17].

- This pipeline is effective but requires the tuning of a number of parameters ;
- It requires significant hardware to be sufficiently fast
- Vessel detection is limited by the vesselness measure, which is not very effective
- It still needs to be evaluated on larger dataset, e.g. full brain vascular network, but annotated data is difficult to obtain.



Step 1: Extracting the vascular network from brain MRA data

- **Filtering**

Improve images (Denoising, contrast enhancement)

- **Segmentation**

Detecting the vascular network

- **Post-processing**

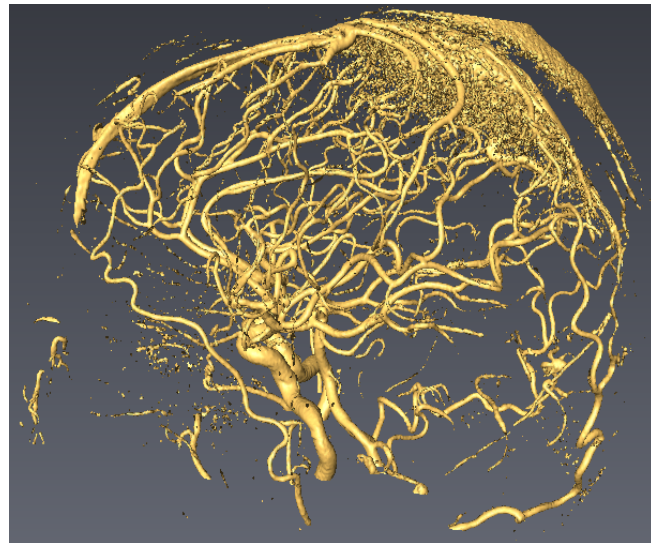
Reconnection, quantitative data analysis: directions, diameter, vessel density ...)



A new filtering method to improve existing segmentation pipeline

2 complementary axes :

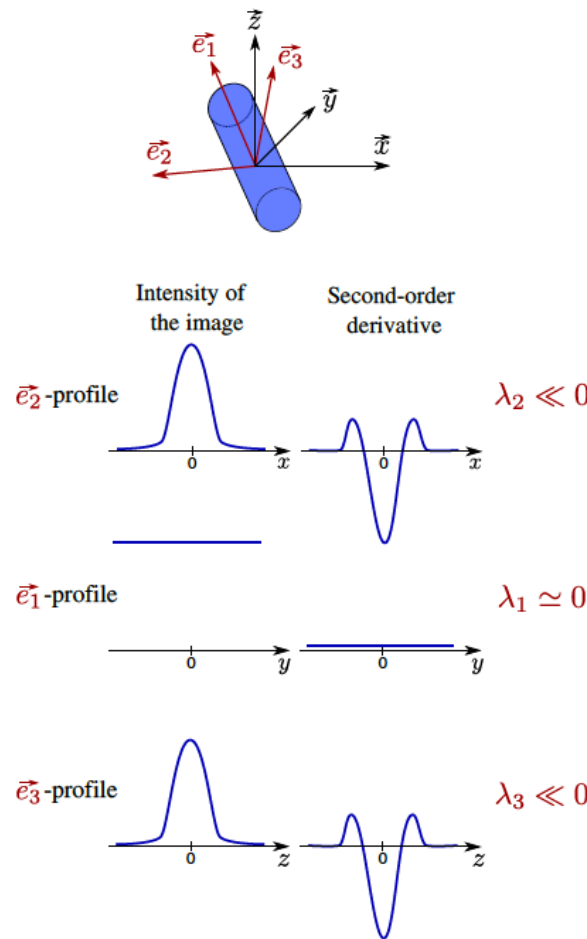
- Noise reduction
- Vascular network contrast enhancement



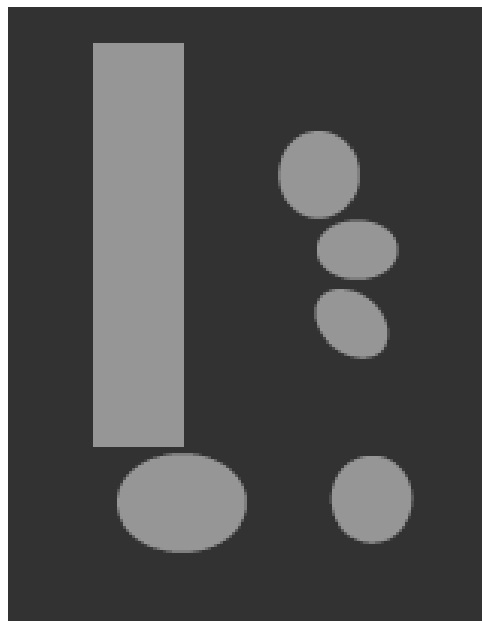
3D MRA data surface rendering



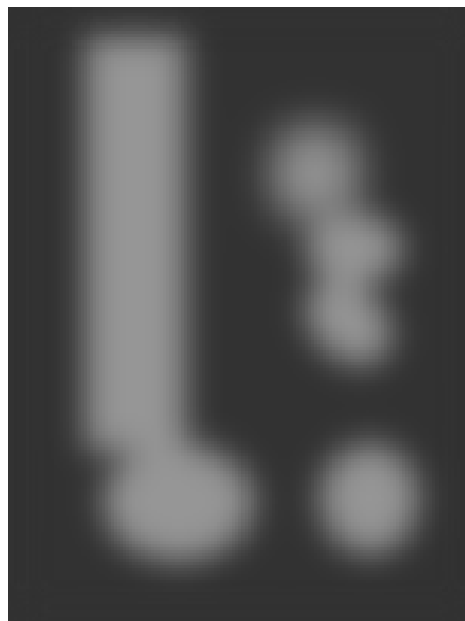
*Maximum intensity
projection*



Classical approach using the Hessian



(a) Initial image



(b) Gaussian filter result

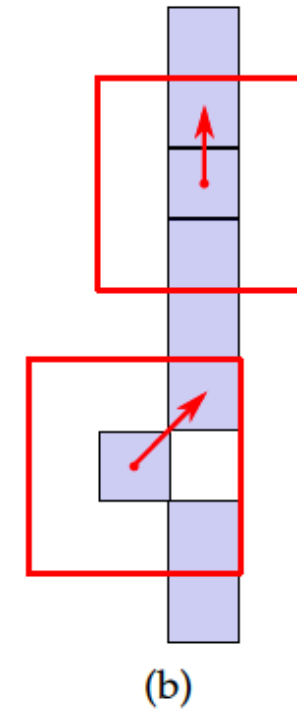
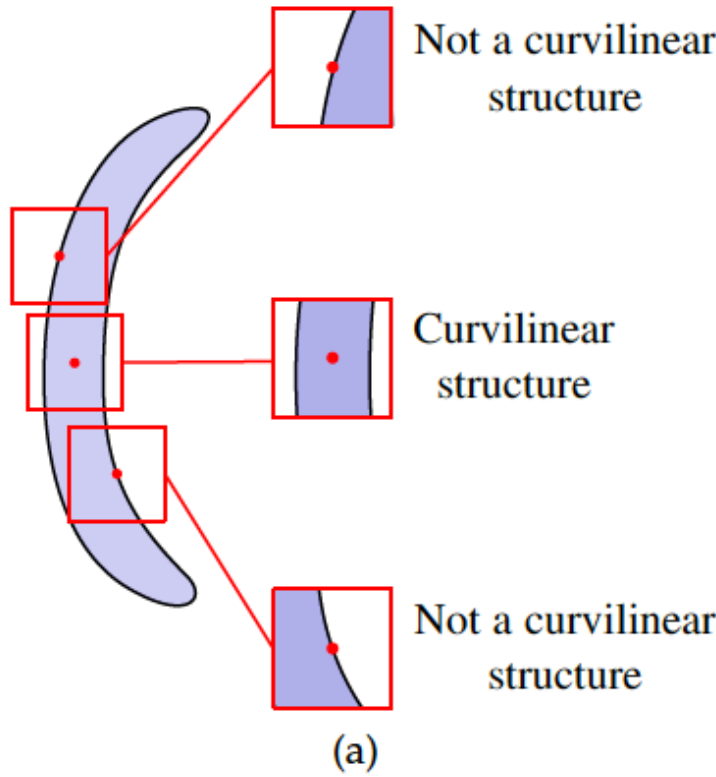


(c) Hessian-based filter re-
sult



(d) Expected result

Scale-space filtering problem



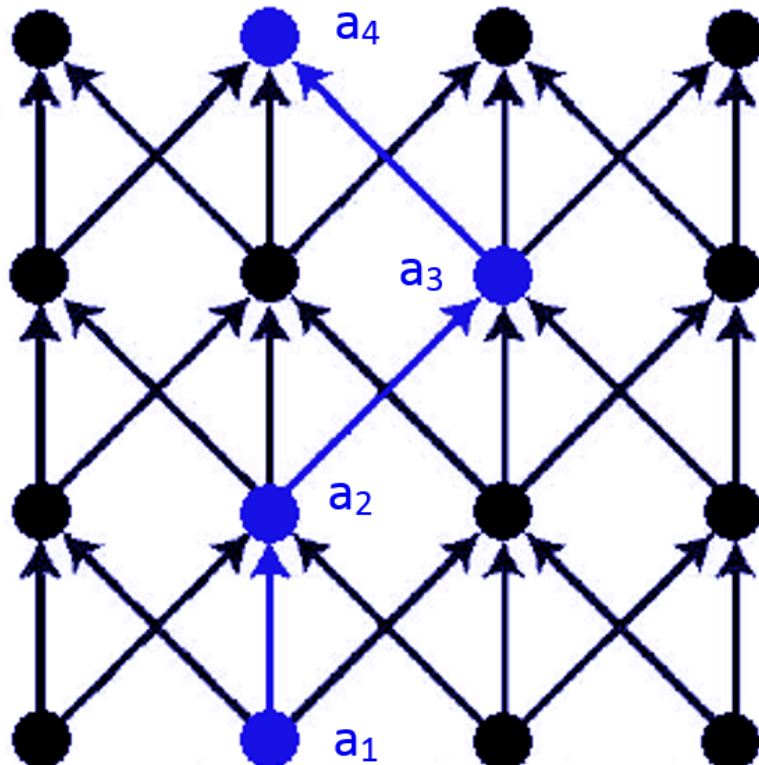
Scale space methods use local neighborhoods and are susceptible to misinterpretation at some scales.



- Scale selection and combination is a challenging problem in traditional scale-space methods.
- One solution is to use semi-local neighborhoods, i.e. that gather information over long distances at all scales.
- We propose the use of paths.

A path, \mathbf{a} , is a set of neighboring pixels on a graph defining an adjacency relation $x \rightarrow y$:

$$\mathbf{a} = (a_1, a_2, \dots, a_L) \quad \text{si } a_k \rightarrow a_{k+1}$$

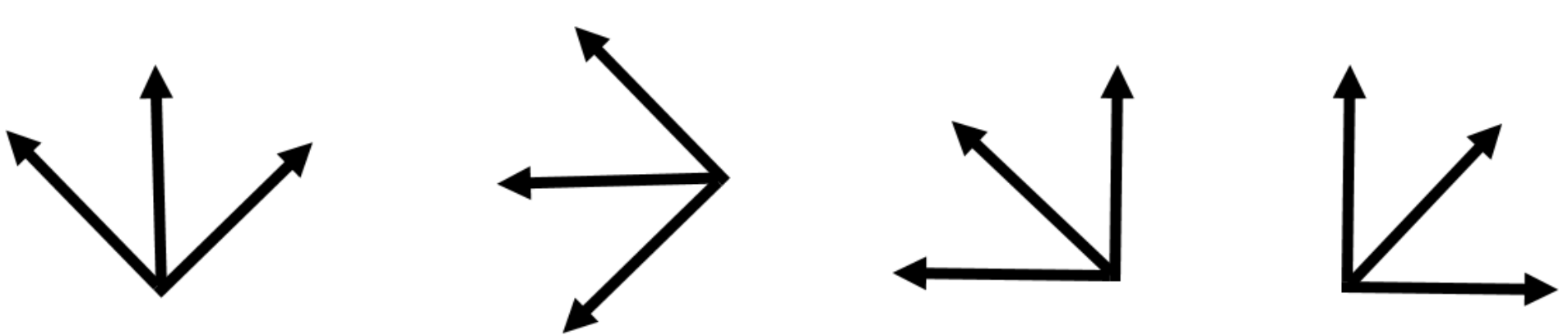


*Adjacency graph (black)
and vertical path \mathbf{a} of length 4
(blue).*



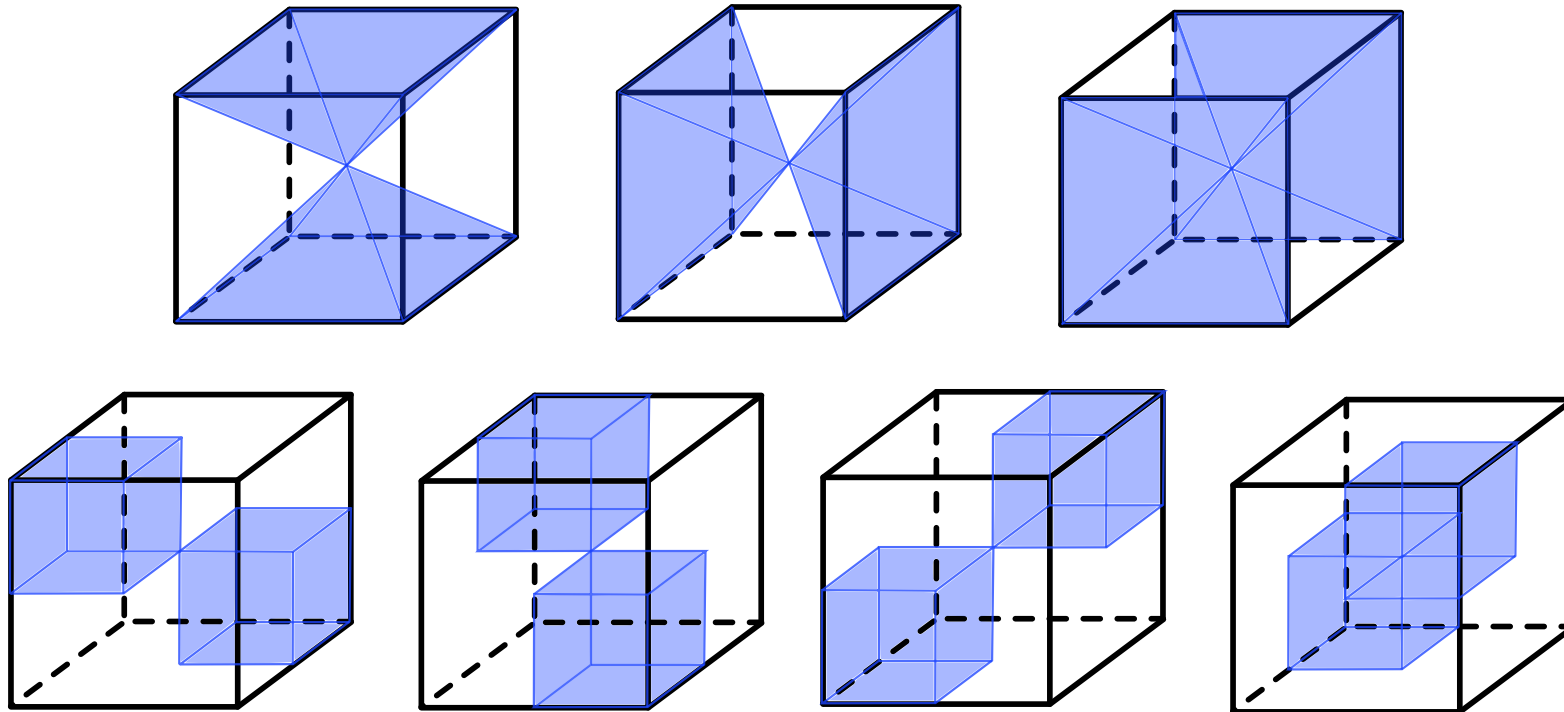
Filtering of an image by a path opening Preserving thin structures in arbitrary orientations imposes to filter the image by several paths each using a particular adjacency graph.

The 2D space is discretized in 4 different orientations :





In 3D, the discrete space is discretized in 7 different orientations :



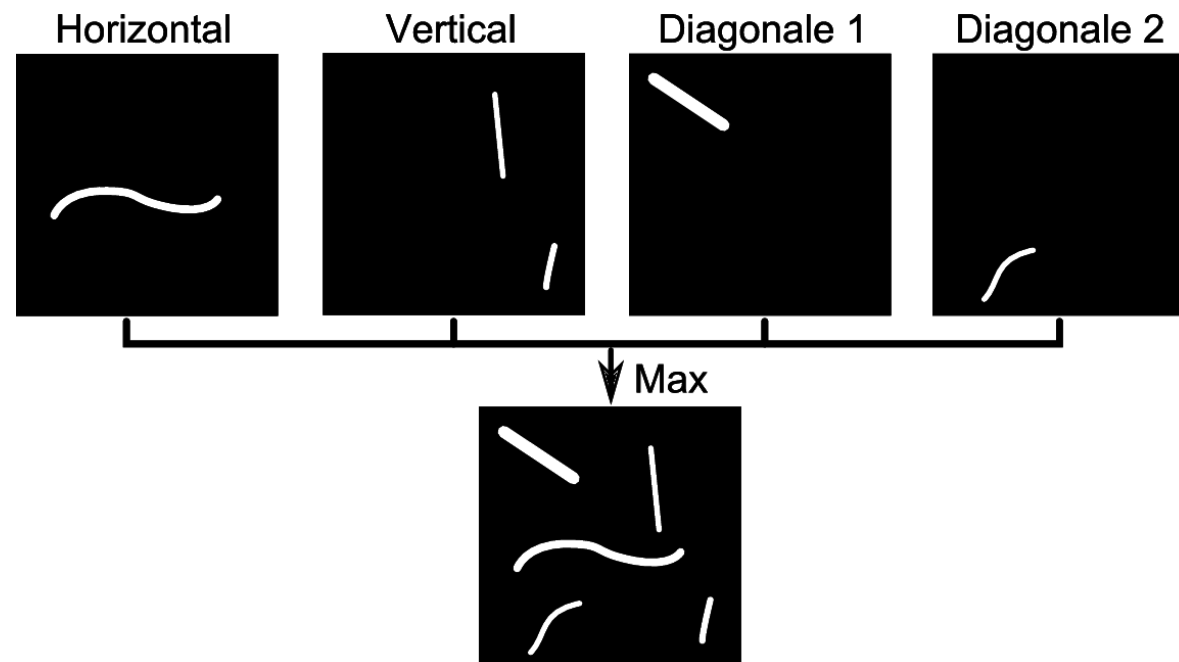


Example binary path opening

$$\alpha_L = \bigvee \{\sigma(\mathbf{a}), \mathbf{a} \in \Pi_L(X)\}$$

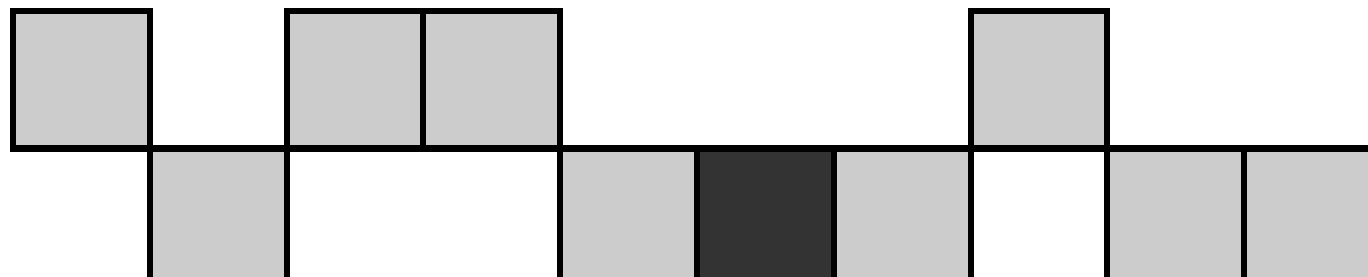
σ_L : Set of all pixels belonging to path \mathbf{a} .

$\Pi_L(X)$: Set of all paths of length L .



Path definition relaxation A path can now admit K consecutive noise pixels between path pixels

This makes it possible to preserve partially disconnected thin/tubular structures :

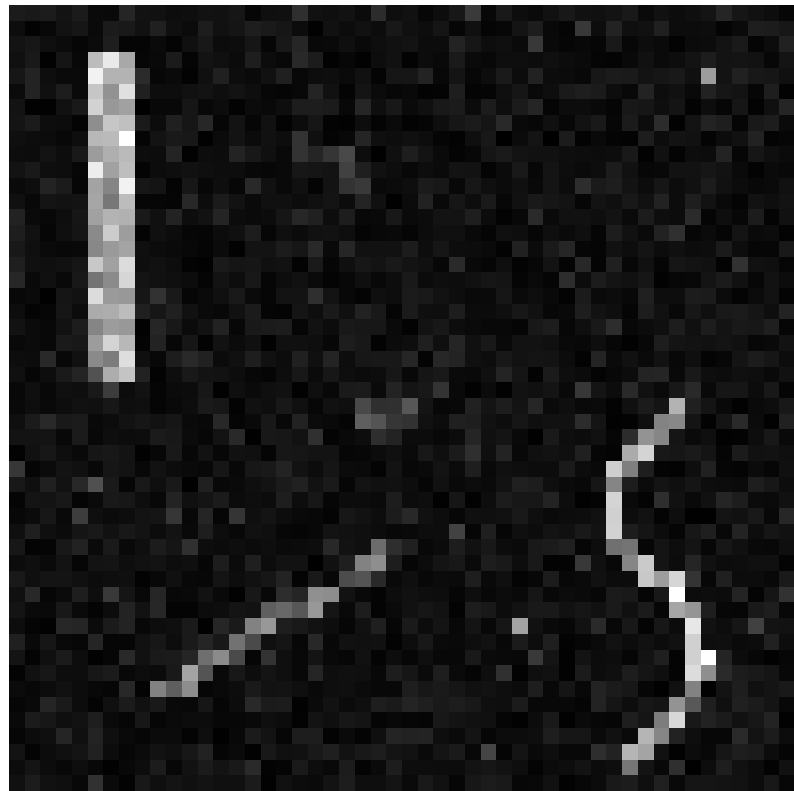


Path with $L = 10$ and $K = 1$ noise pixel

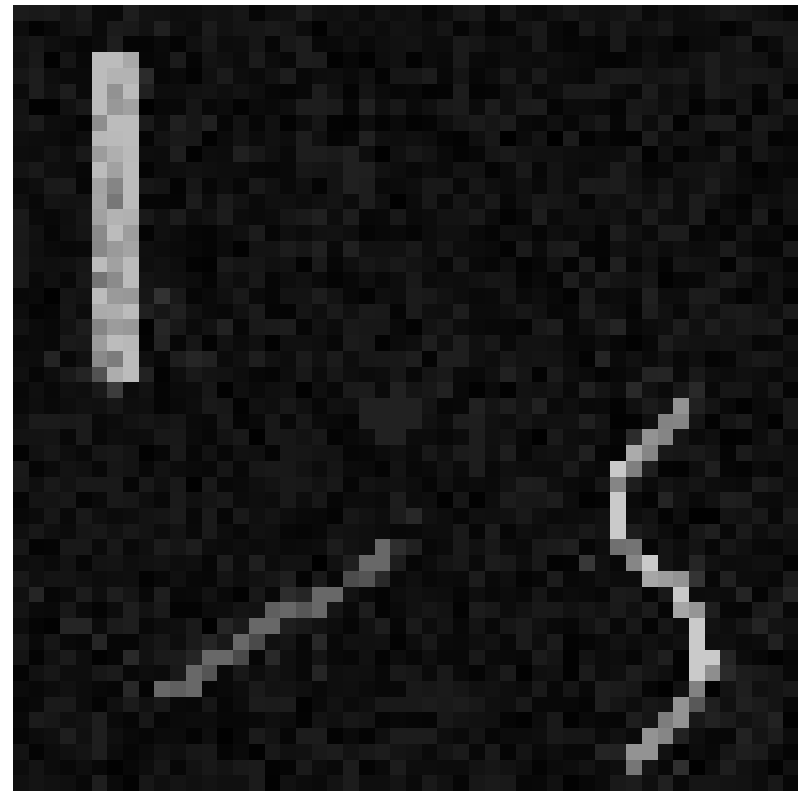
This notion is different from that of *path incompleteness* by Heijman et al, it was proposed by F. Cokelaer [5] and is simpler to implement.



RPO Example on a synthetic, noisy 2D image (AWGN mean = 0, $\sigma = 20$:



Initial image 50x50px

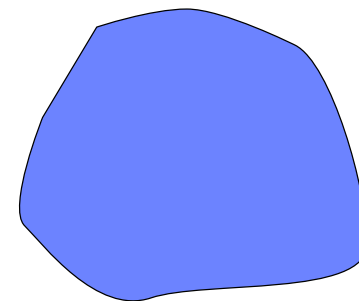


RPO L=10, K=1



2D Case 2 Types of structures :

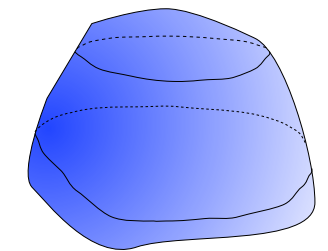
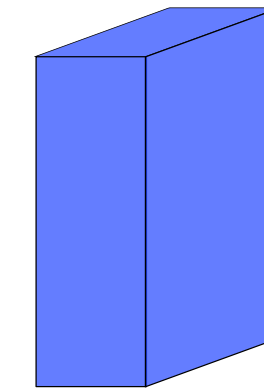
Fibres and Blobs



RPO preserves only fibres if blobs are not too big.

3D Case 3 Types of structures :

Tubes, Planes and Blobs



RPO preserves both tubes and planes.

An RPO by itself preserves more than just tubes in 3D images. Another filter is thus necessary to eliminate planar structures.

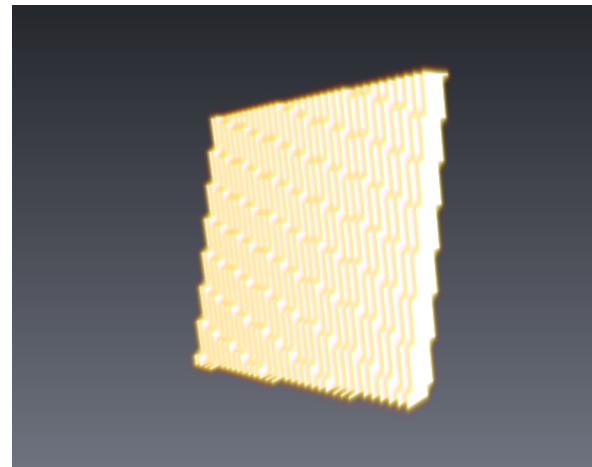


Hypothesis Planar structures should be detected in at least one more orientation than tubular structures

Test of this hypothesis on 3 synthetic structures :



Tube



Plane

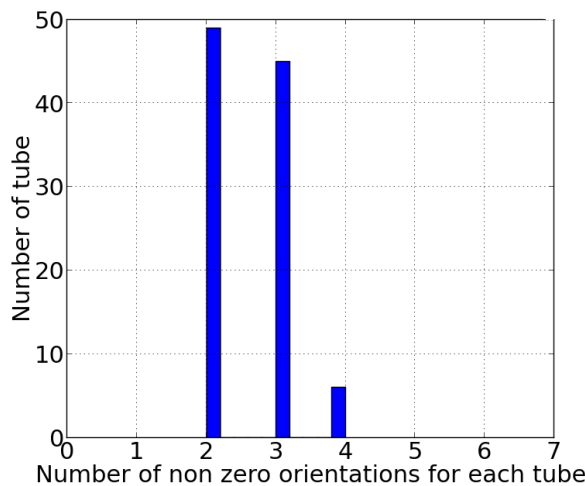


Half-ellipsoid surface

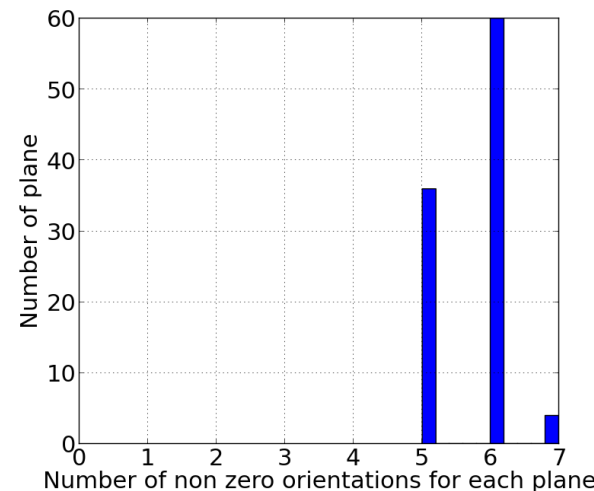


Test : Filtering 100 3D images of each structure and measuring the number of RPO orientations still containing the structure after filtering

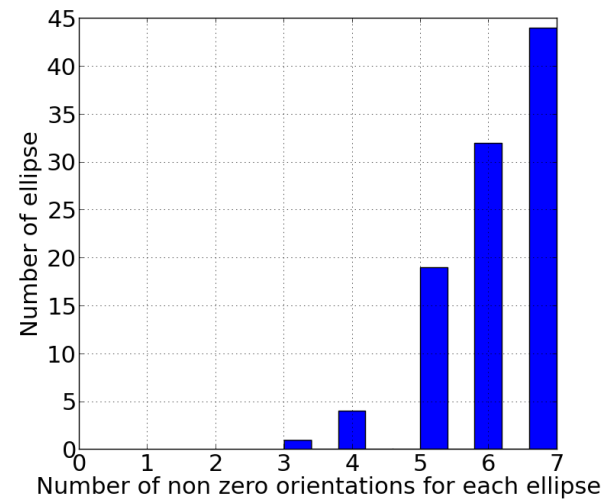
Histogram of the number of orientations preserving the synthetic structure:



Tubes



Planes



Half-ellipsoids

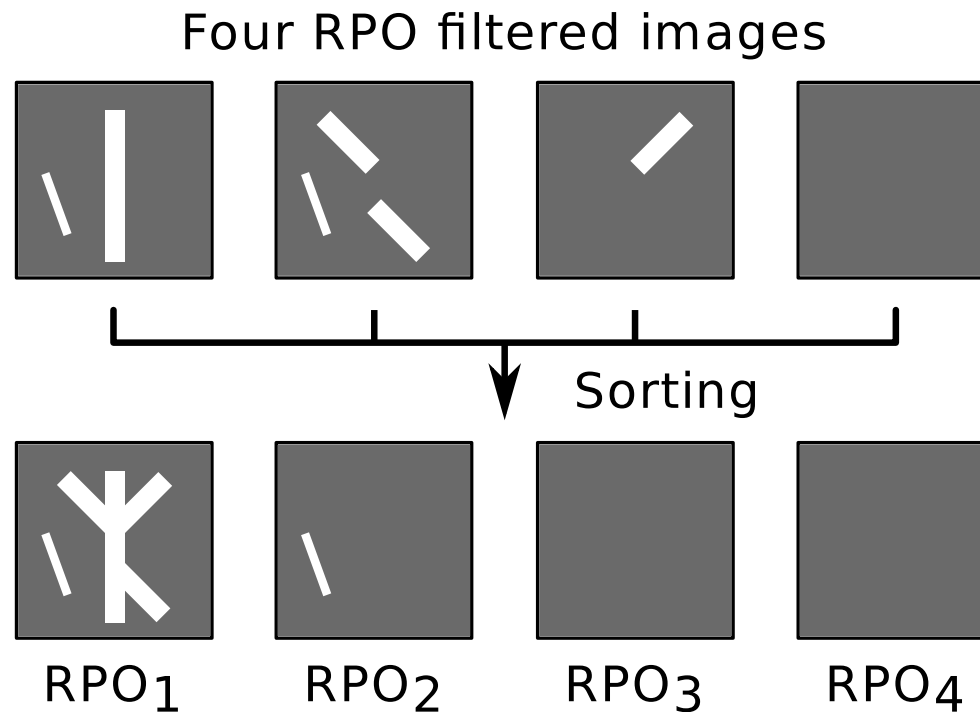
New operator

We order the result of each RPO orientation pixelwise and compute

$$\text{RORPO} = \text{RPO}_1 - \text{RPO}_i$$

RPO_1 : Result of standard RPO (max of all RPOs)

RPO_i : The $i - th$ rank of the RPO.

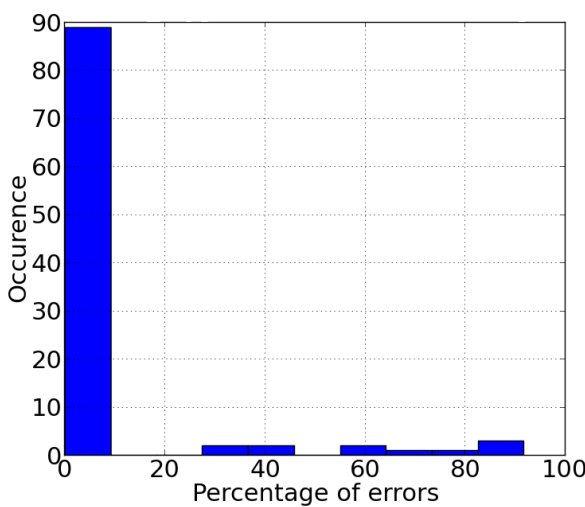




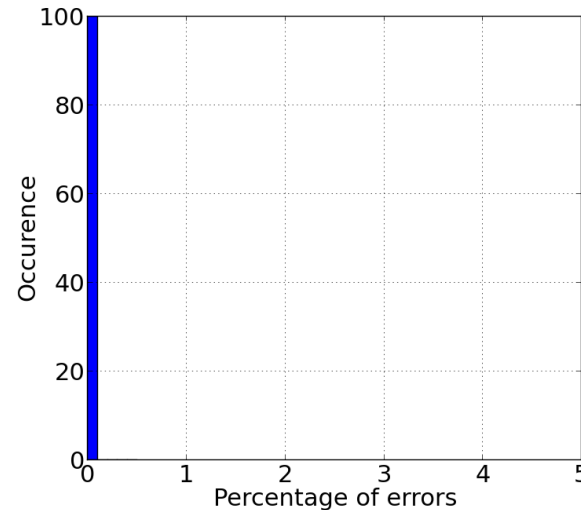
We compute the RORPO error rate on 100 random synthetic structure of each type.

$$\%error = \frac{nb_{error}}{nb_{pixels}} \times 100$$

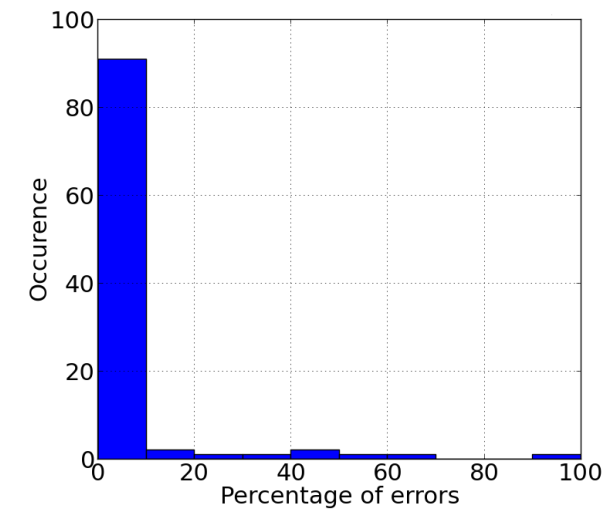
nb_{error} : number of false negative pixels for the tubes and of false positifs for the planes and half-ellipsoids.



Tubes ($m = 4\%$)



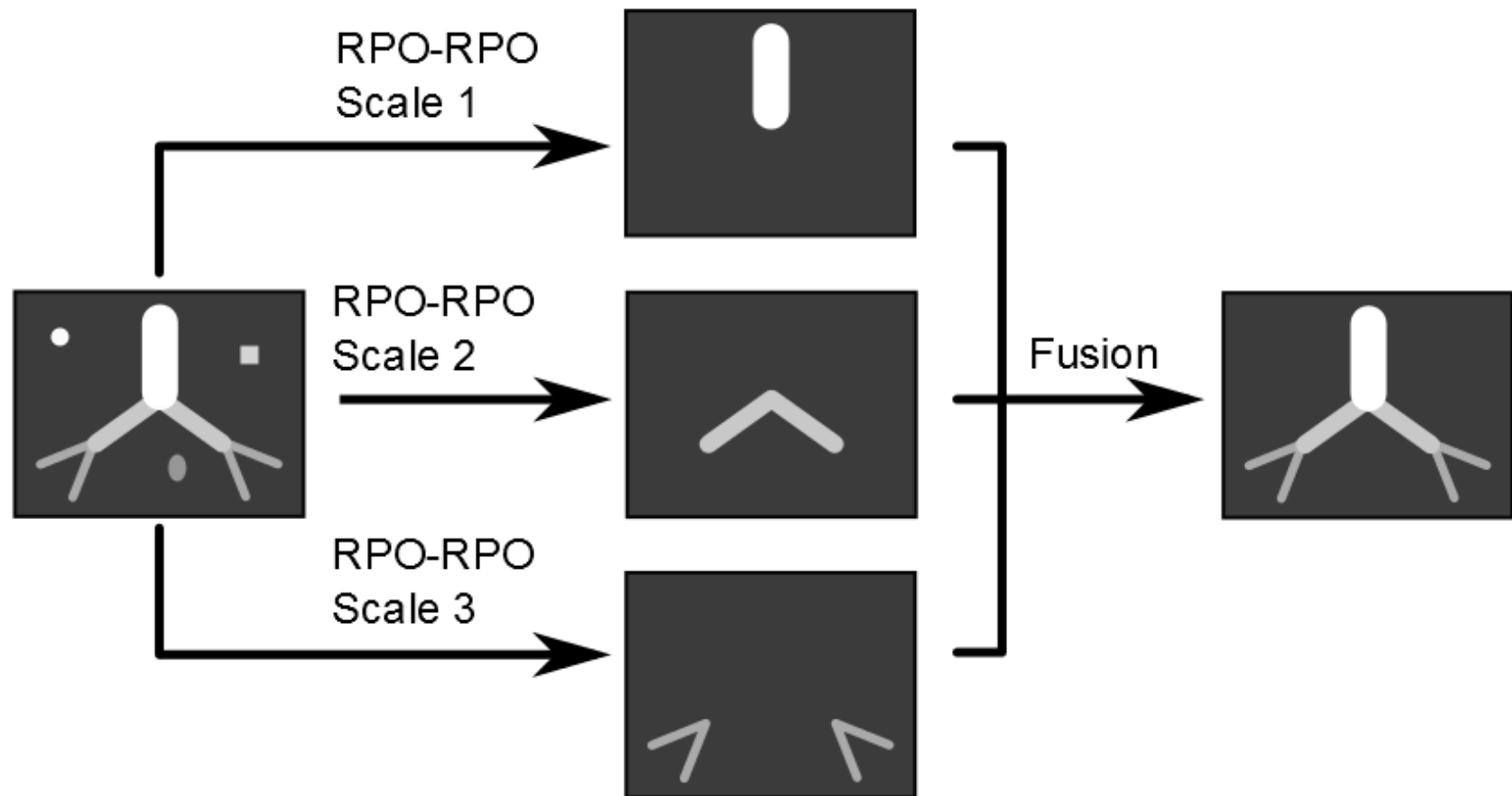
Planes ($m = 0\%$)

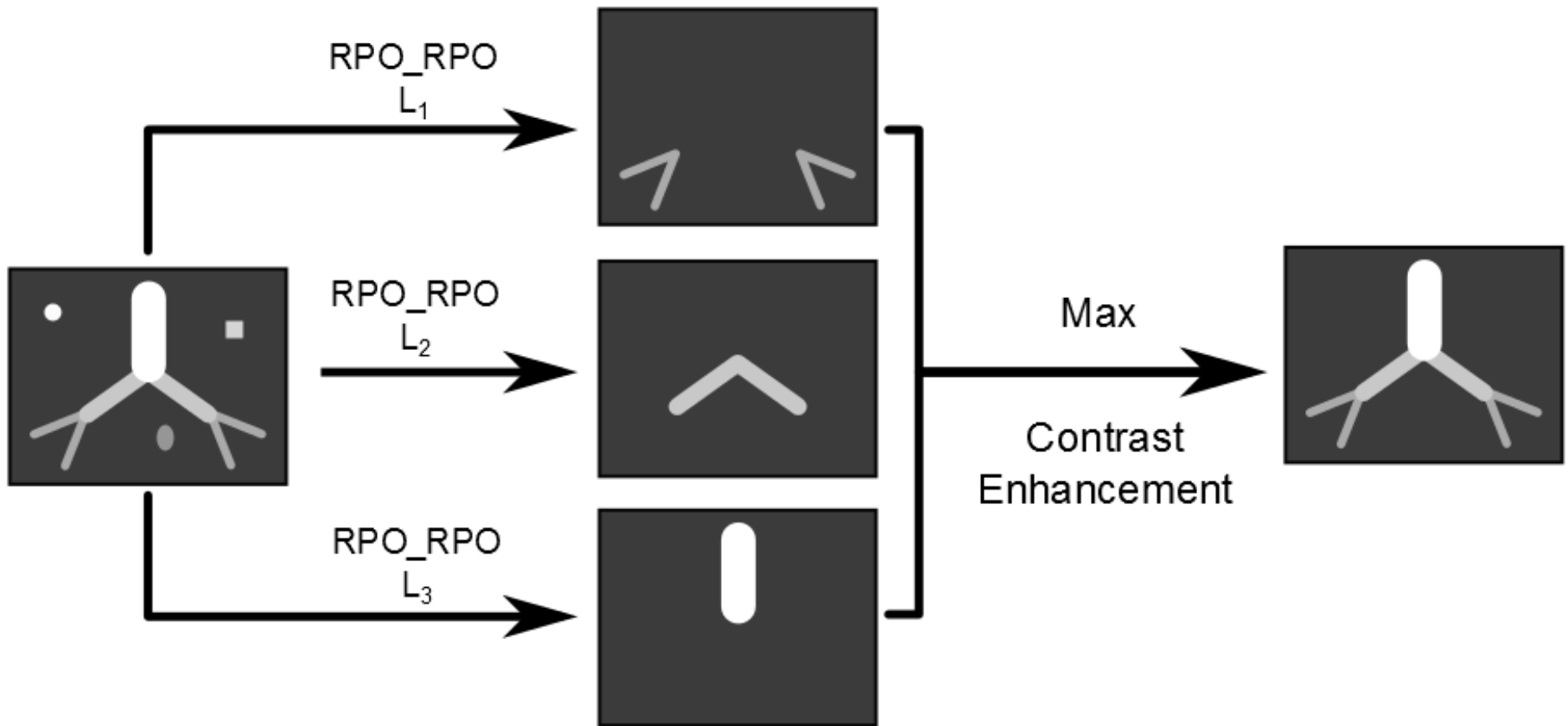


Half ellipsoids ($m = 4\%$)



What is a multi-scale approach ?





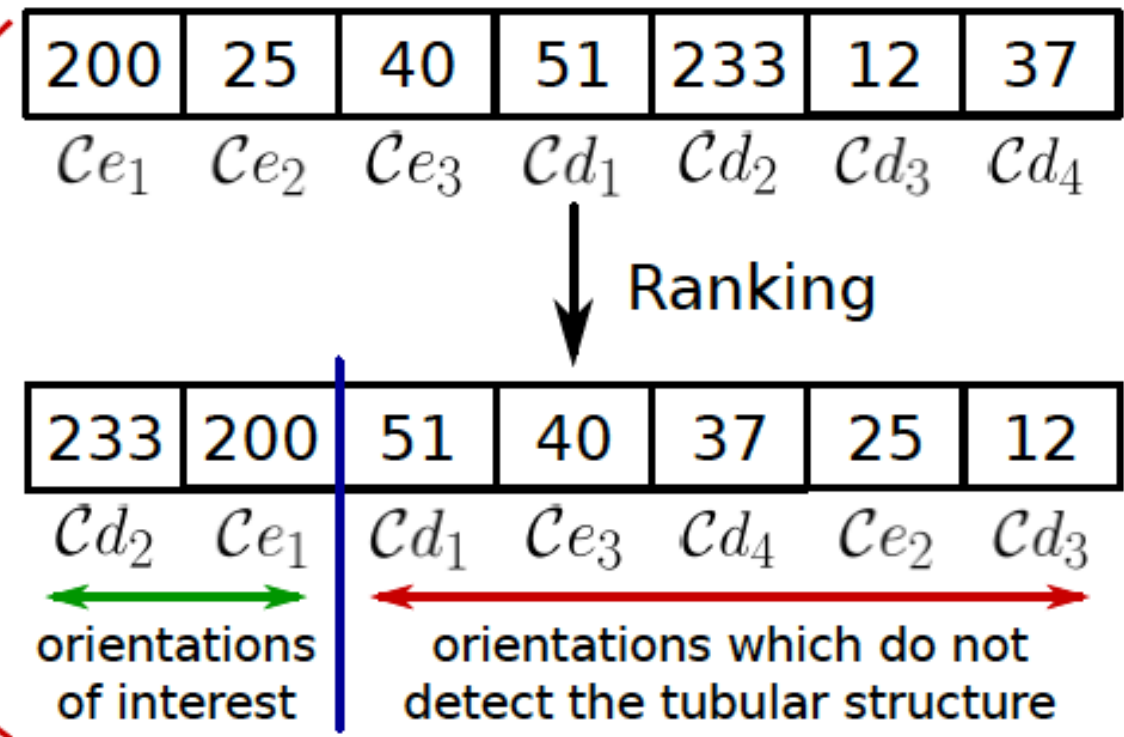
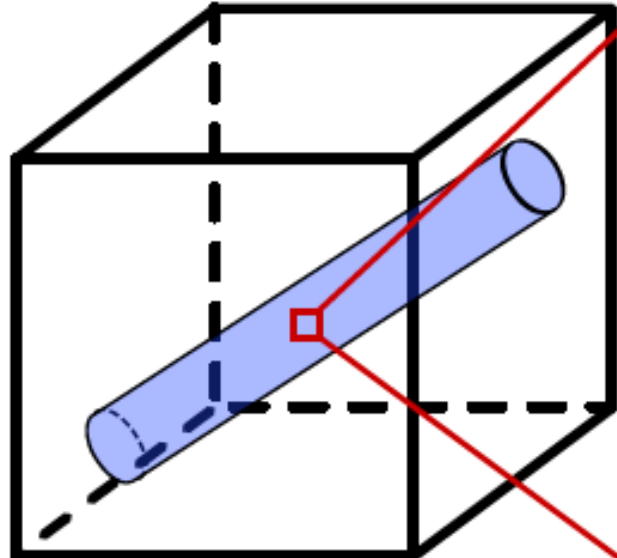
We performed qualitative comparisons of various methods according to four criteria on a full cerebral MRA

- Capacity to reduce background noise
- Capacity to detect large blood vessels
- Capacity to detect small blood vessels
- Presence of artifacts

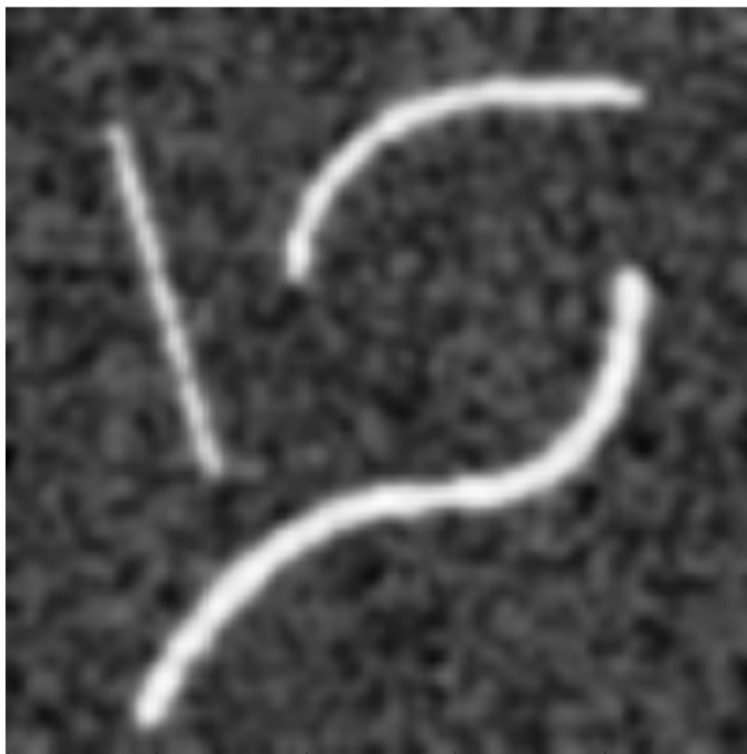
RORPO with classical adjacencies and a multiscale approach based on path lengths seems to provide the best compromise.



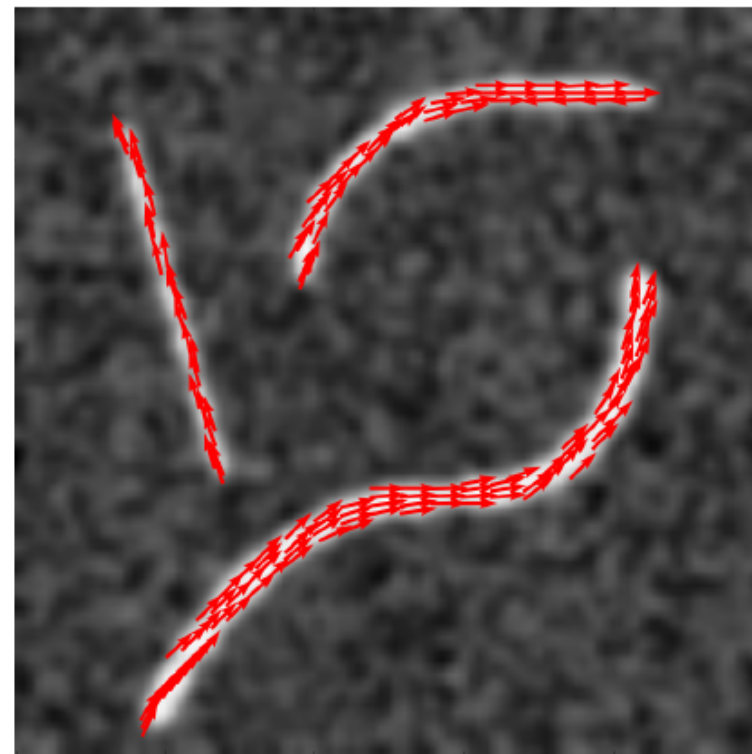
Computing directions from RORPO



Computing directions from RORPO can be done by averaging the directions of high response.



(a)

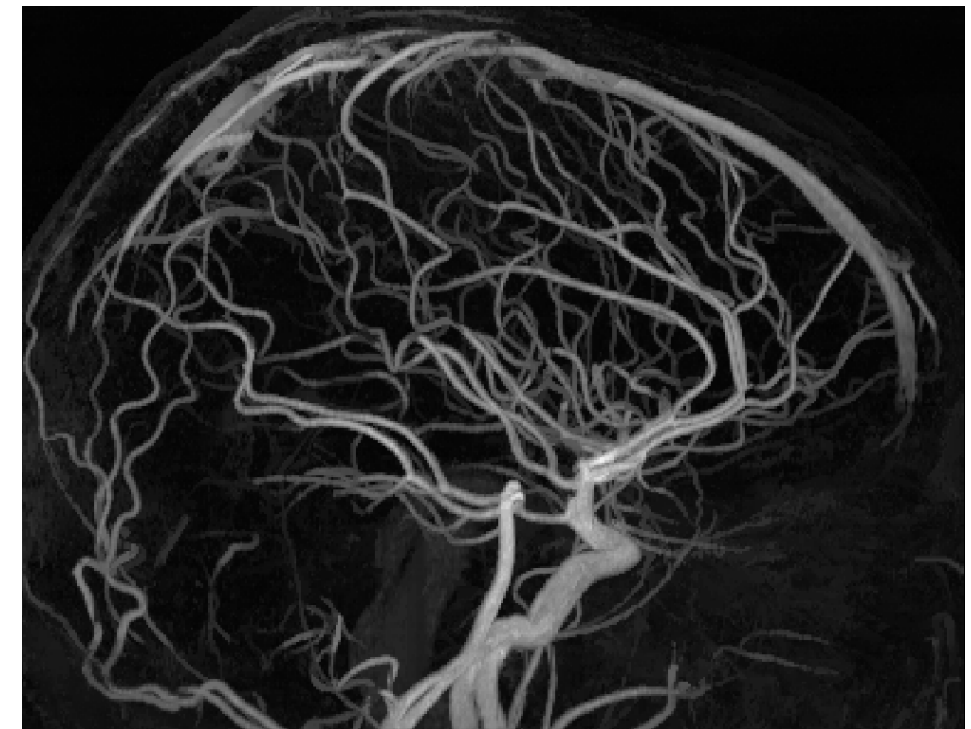


(b)

Orientation feature in 2D



Initial image MIP



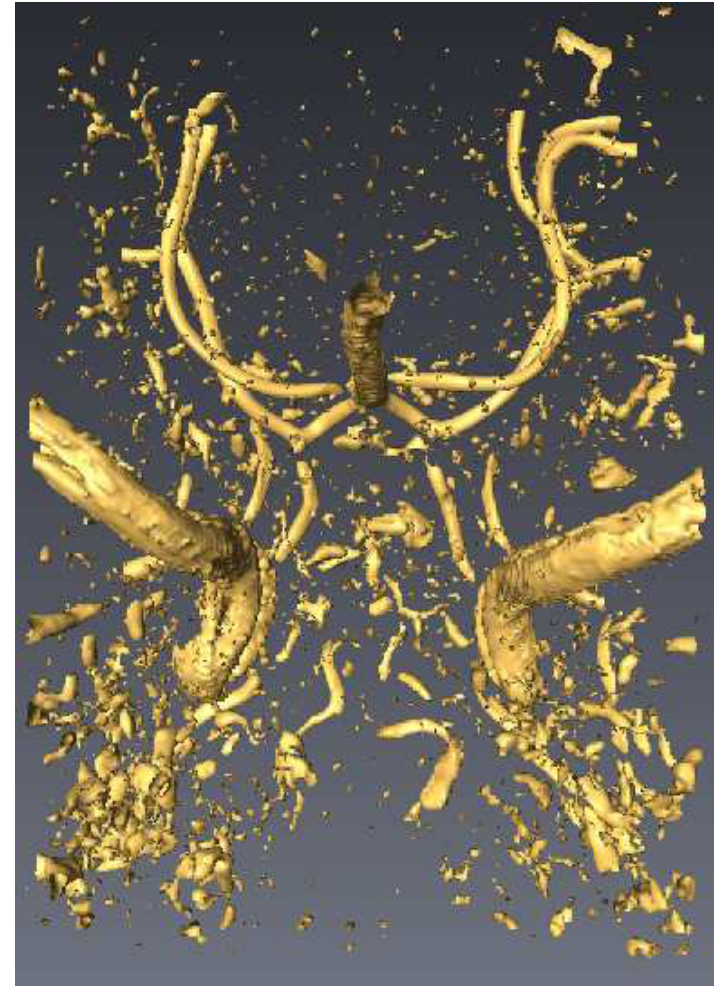
Length-based multiscale RORPO



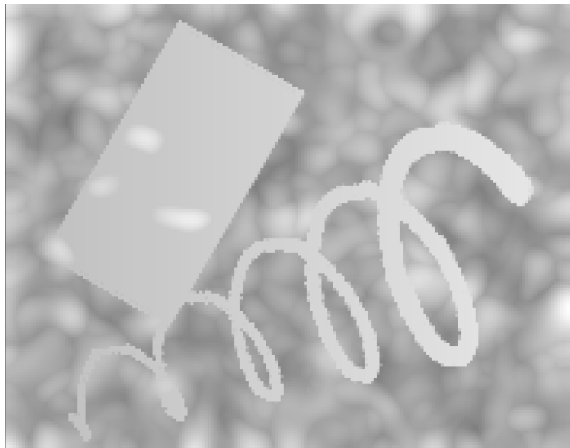
Comparison with Frangi vesselness



Proposed method



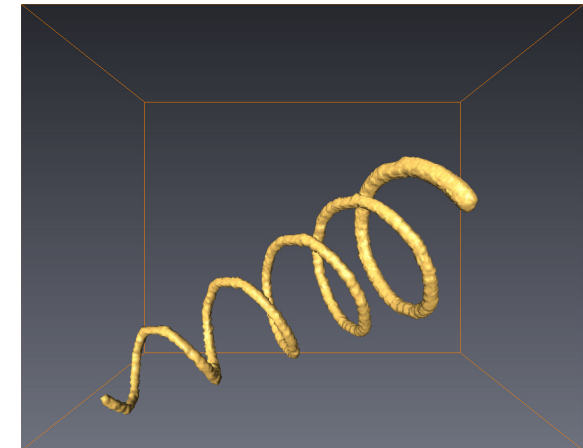
Optimized Frangi vesselness



(a) CCM=0.605,
Dice=0.634



(b)

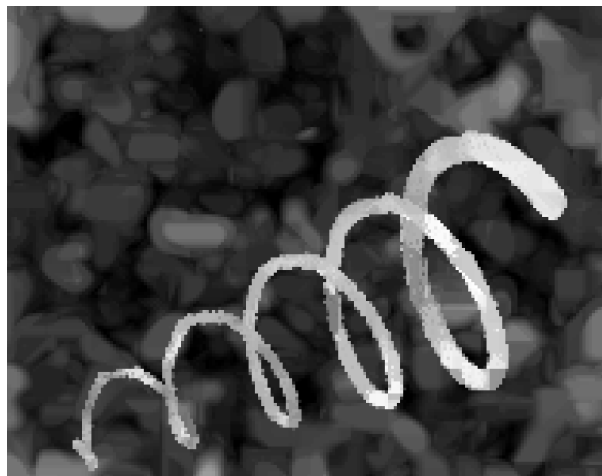


(c)

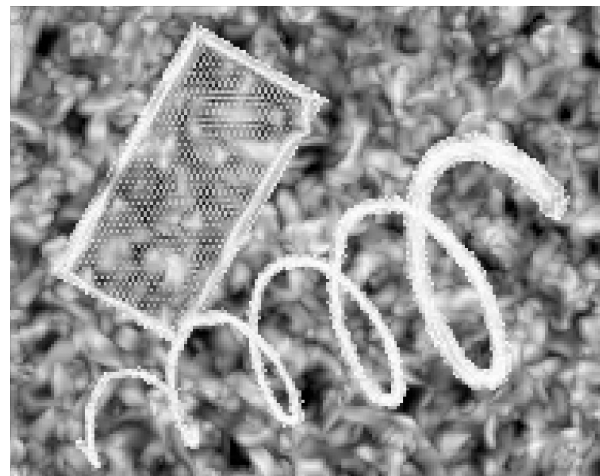
*Synthetic image: (a) maximum intensity projection and (b) isosurface.
(c) Ground truth.*



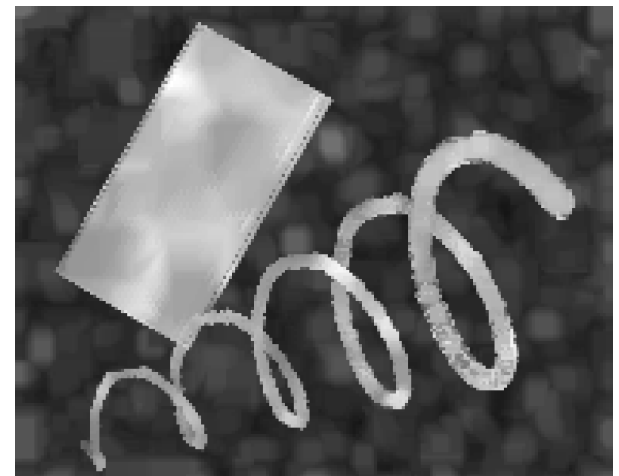
Filtering response



(a) CCM=0.884, Dice=0.893

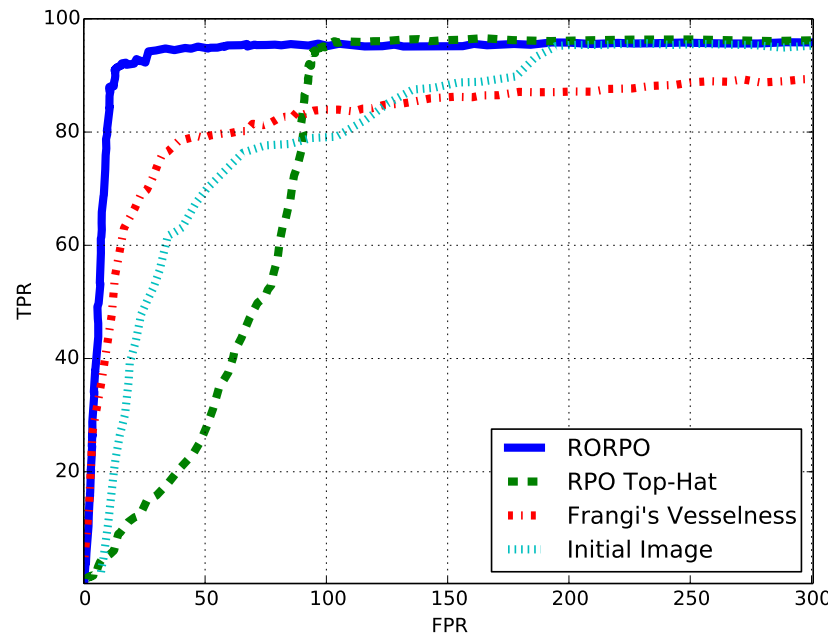


(b) CCM=0.706, Dice=0.730

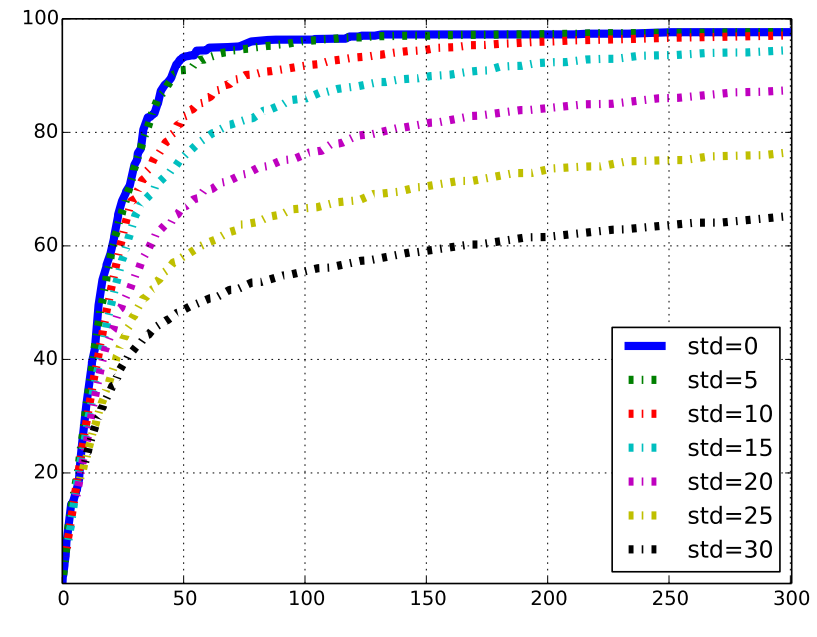


(c) CCM=0.655, Dice=0.654

*Filtered synthetic image: maximum intensity projection. (a) RORPO.
(b) Frangi's vesselness. (c) and RPO-top-hat.*



(d)

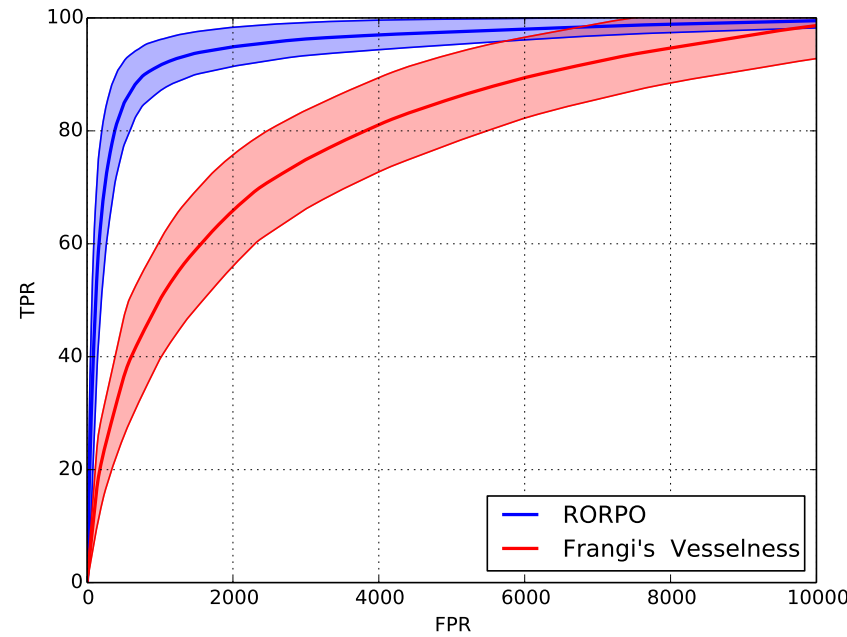


(e)

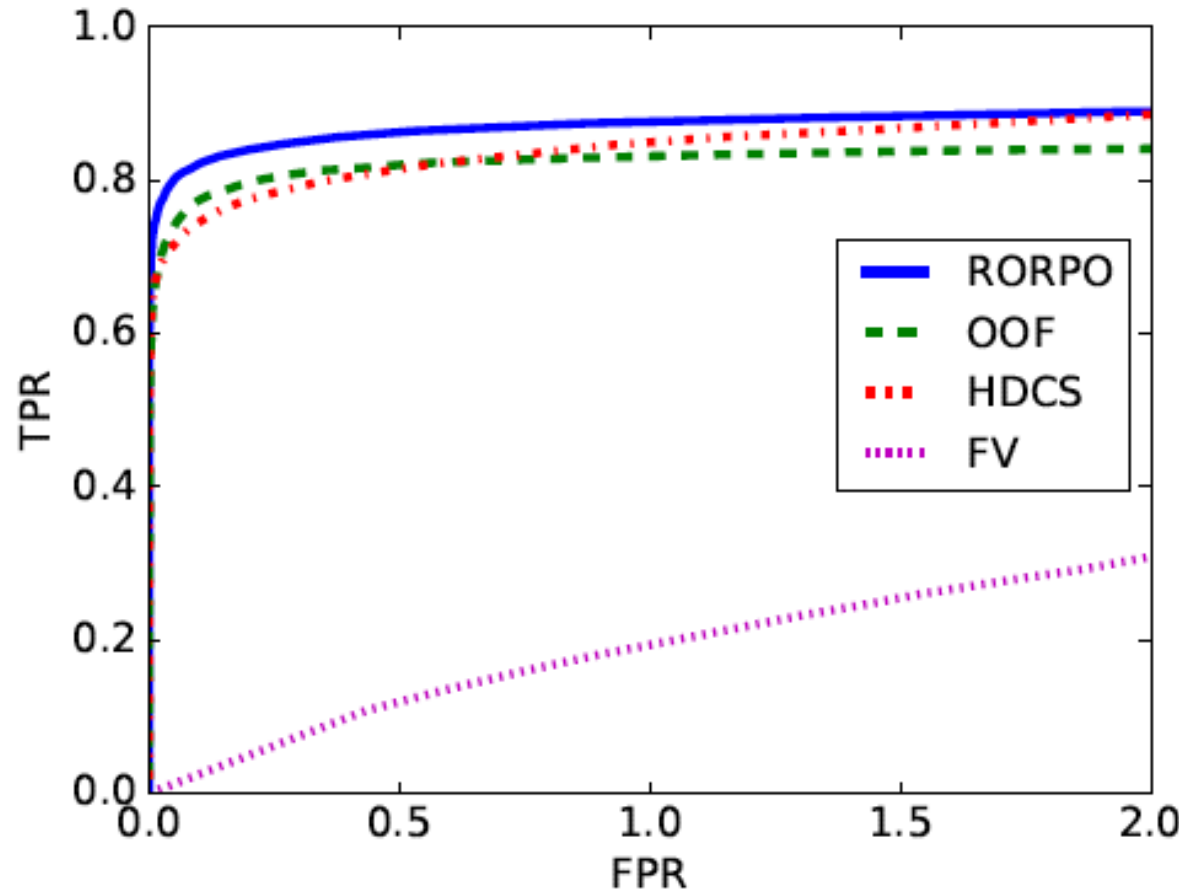
ROC curves on synthetic data. (a) Comparison of the three filters, plus the native image. (b) Noise robustness of the RORPO filter.



MICCAI Rotterdam Coronaries Database



ROC curves of RORPO and Frangi's Vesselness on the Rotterdam repository. For both filtering the central curve is the mean ROC curve and the two others are the mean plus or minus one standard deviation ROC curve.



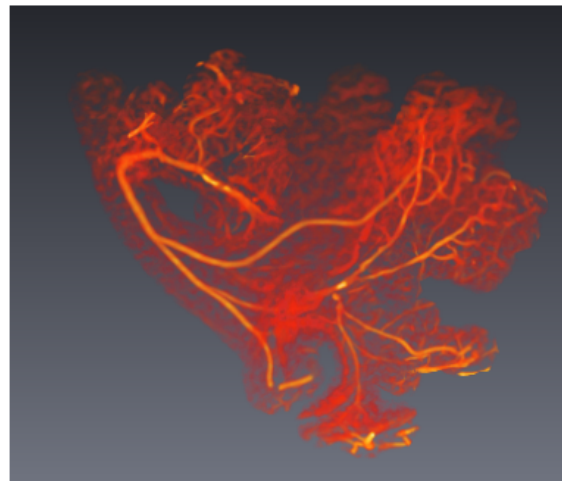
Three-way ROC analysis RORPO vs. OOF [11],
HDCS [13] and Frangi Vesselness (FV)



(a)



(b) $\text{MCC} = 0.541$

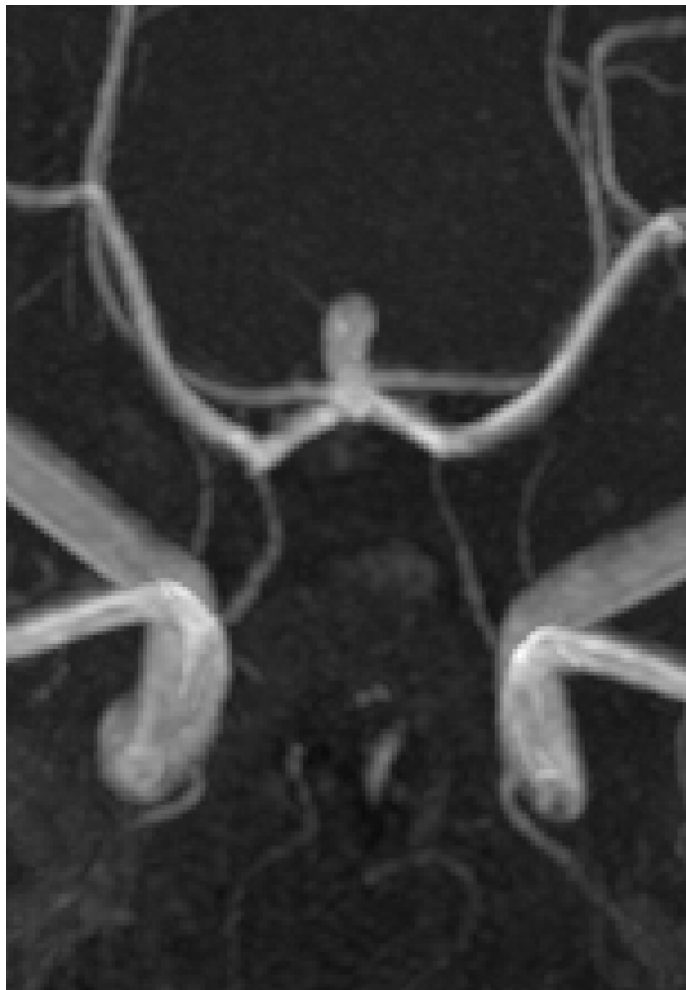


(c) $\text{MCC} = 0.529$



(d) $\text{MCC} = 0.405$

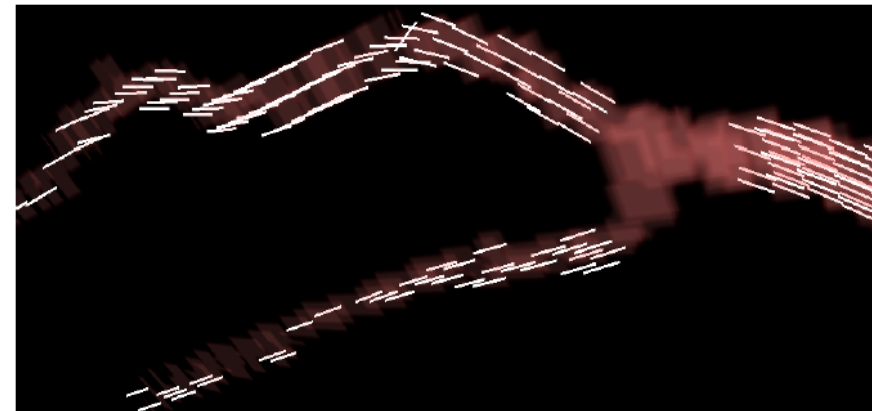
Ground truth (a) : RORPO (b), OOF [11] (c), Frangi (d)



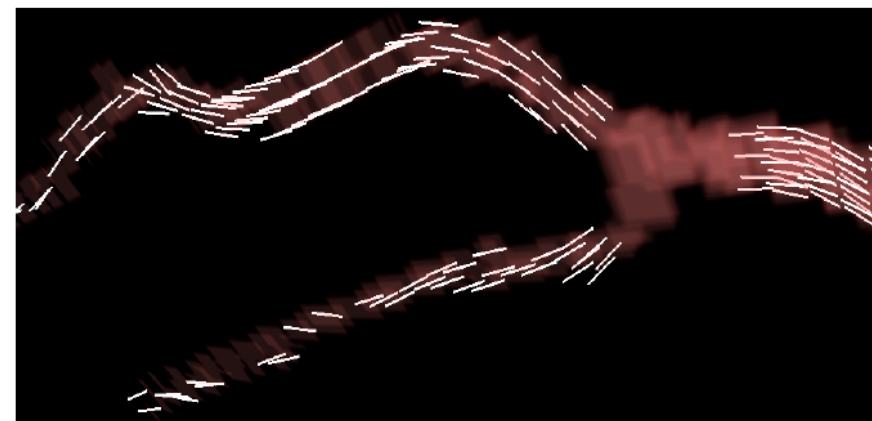
Initial image



Multiscale RORPO



(a)



(b)

Orientation feature in 3D, Heart data: RORPO (a)
vs Frangi Vesselness (b)

- So far we have proposed a solution for curvilinear structure filtering.
- Segmentation of more complex structures that include tubes/cylinders can be built from this.
- We propose to use a variational framework by improving Total Variation (TV) to include a directional component.

We consider a convex variational framework

$$\min_{u \in X} F(u, f) + \lambda G(u). \quad (6)$$

- Here F is a data fidelity term and G a regularization.
- f is the input data and u the desired result.
- Typically F is associated to a noise model and G to an image model.
- A common image model is the Total Variation (TV)



This is isotropic standard TV regularization term (in 2D):

$$\text{TV}(u) = \|\nabla u\|_{2,1} = \sum_{0 \leq i,j < N} \sqrt{((\nabla u)_{i,j}^x)^2 + ((\nabla u)_{i,j}^y)^2} \quad (7)$$

where $\nabla u = ((\nabla u)^x, (\nabla u)^y)$ is the 2D gradient.

It is classical in mathematics, and was proposed for image regularization in [18] (ROF model).



We define a directional gradient, $\nabla_D \in X^p$:

- We first define a *span* (v_1, \dots, v_p) of p unitary vectors.
- This span contains all the discrete undirected orientations in a $k \times k$ neighborhood
- then:

$$\nabla_D u = \left(D^1 \circ (\nabla_d u)^1, \dots, D^p \circ (\nabla_d u)^1 \right) \quad (8)$$

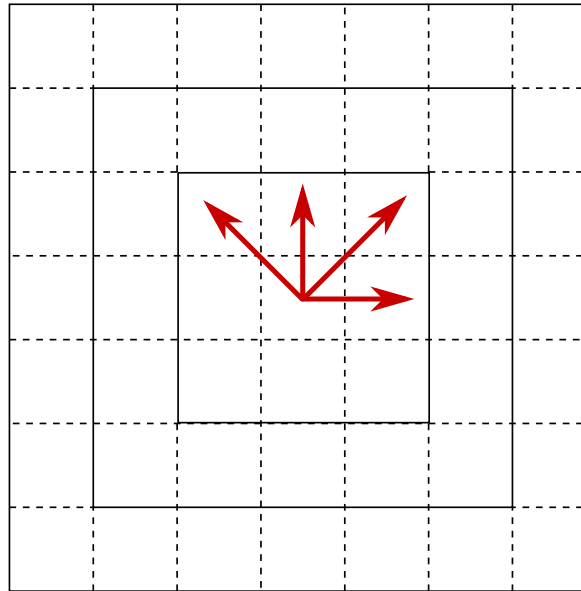
$$(\nabla_D u)_{i,j} = D_{i,j}^1 (\nabla_d u)_{i,j}^1 v_1 + \dots + D_{i,j}^p (\nabla_d u)_{i,j}^p v_p \quad (9)$$

- with $D^q \in X$, $1 \leq q \leq p$ a weight image such that:

$$D_{i,j}^q = d_{i,j}^q \Phi_{i,j} + (1 - \Phi_{i,j}) \quad (10)$$

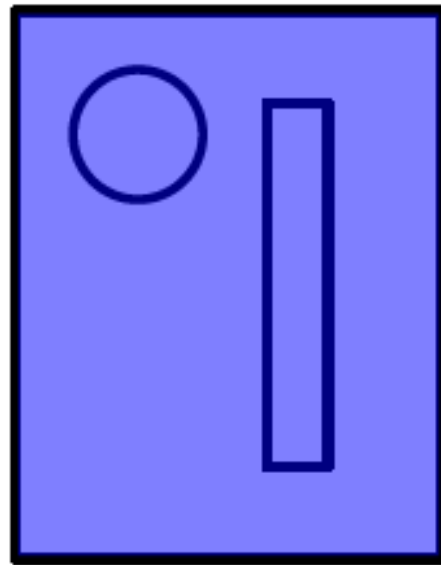


- $\Phi \in X$ is a vesselness-like intensity feature normalized to the interval $[0, 1]$
- $(d^i)_{i \in \llbracket 1, p \rrbracket}$, are computed from an orientation field

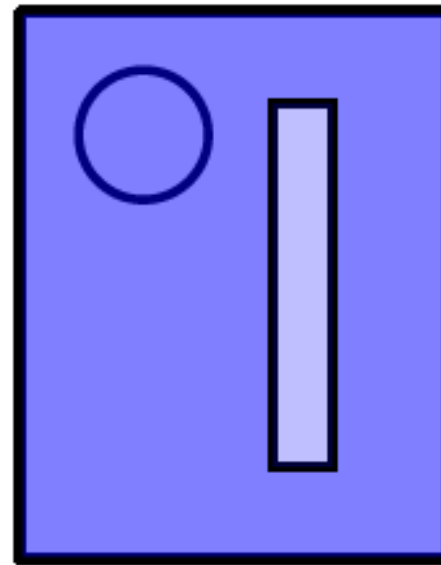


Span of vectors in a 3×3 neighborhood.

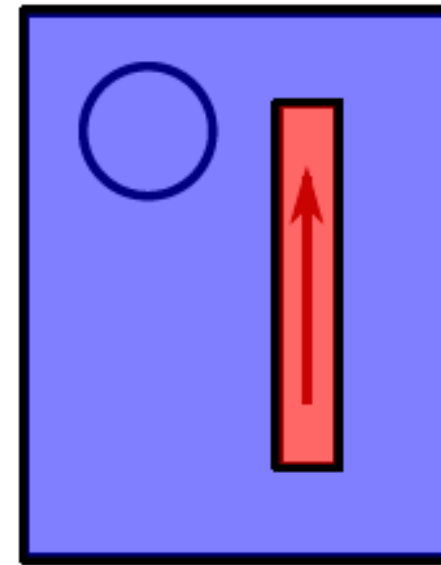
We used the RORPO response as the vesselness feature and the orientation field computed from RORPO.



(a) TV



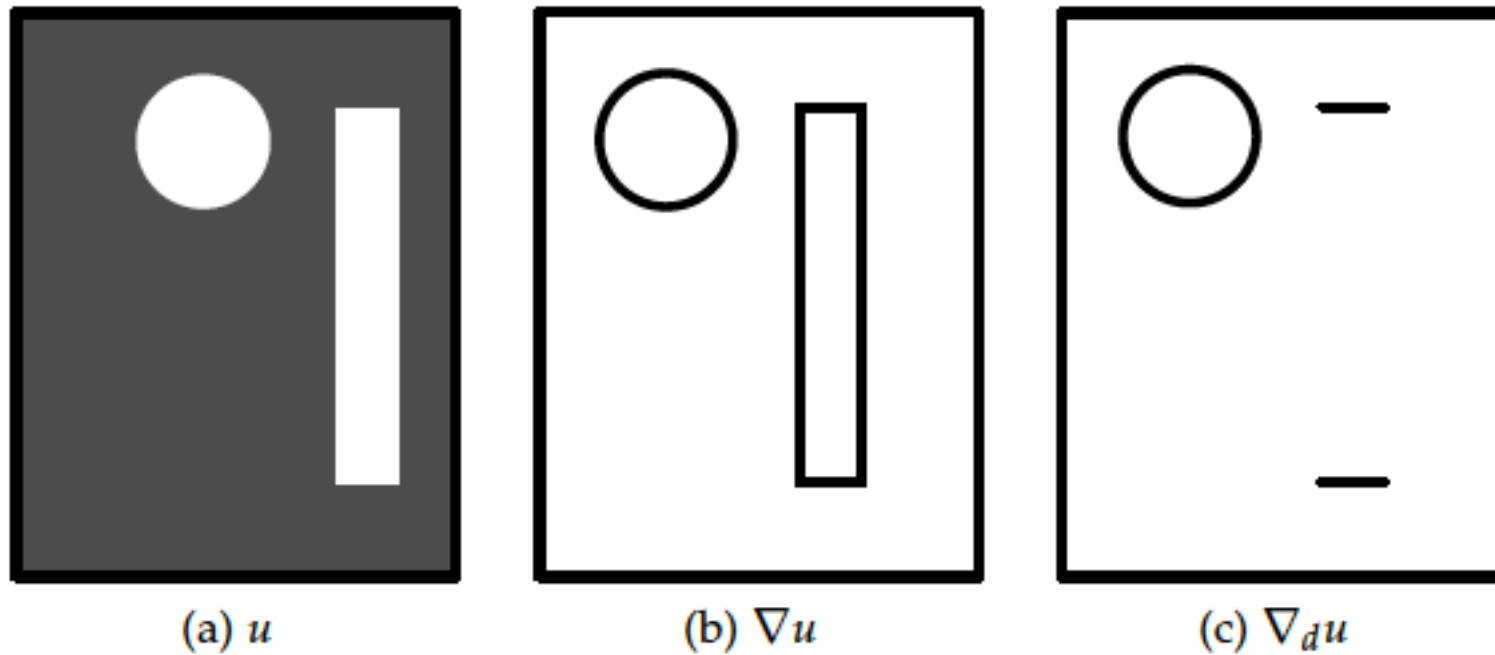
(b) Weighted TV [6o]



(c) Directional TV

Directional TV idea

- Standard TV will penalize all edges identically; weighted TV may attempt to penalize edges less in a curvilinear object.
- A directional feature will not penalize edges inside a curvilinear object



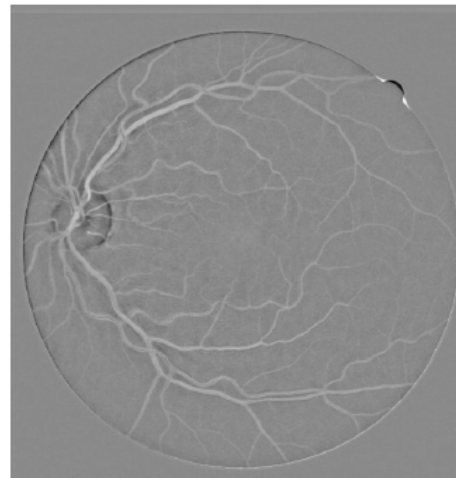
Theoretical edge weights

- Thin, curvilinear object are all edges, and so are easily filtered out in standard/weighted TV.
- A directional TV will filter only along the direction of the curvilinear object, preserving it.

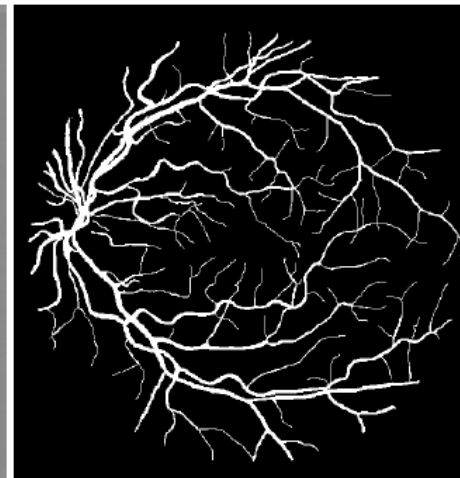
Our model is base on TV_D , as follows:

$$\underset{u \in [0,1]^{N \times N}}{\text{minimize}} \quad \langle c_f, u \rangle_F + \lambda \|\nabla_D u\|_{2,1} \quad (11)$$

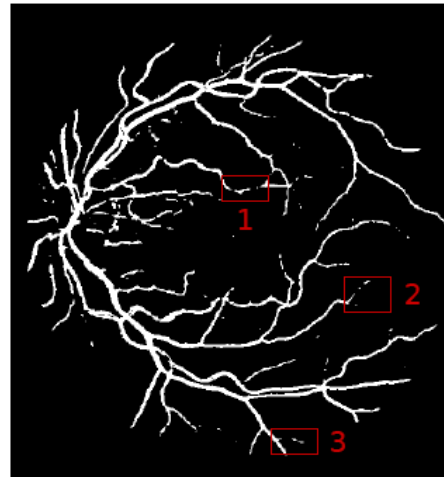
- $\|\nabla_D u\|_{2,1}$ is the directional Total Variation
- $\langle c_f, u \rangle_F$ is the Chan et al. data fidelity term [3] where $(c_f)_{i,j} = (c_1 - f_{i,j})^2 - (c_2 - f_{i,j})^2$ and $\langle u, v \rangle_F$ is the Frobenius product.
- The scalars c_1 and c_2 are respectively the foreground and background constant and f is the initial image.



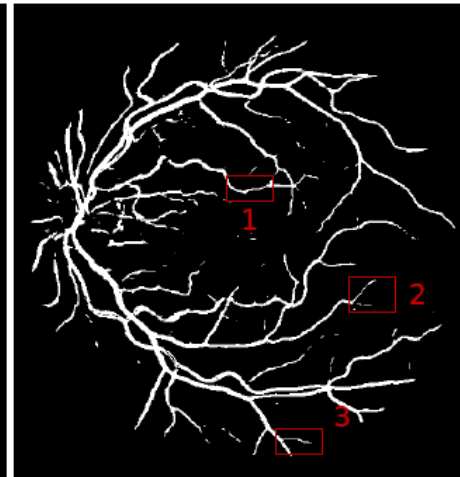
(a) Background corrected initial image



(b) Ground truth



(c) Chan model

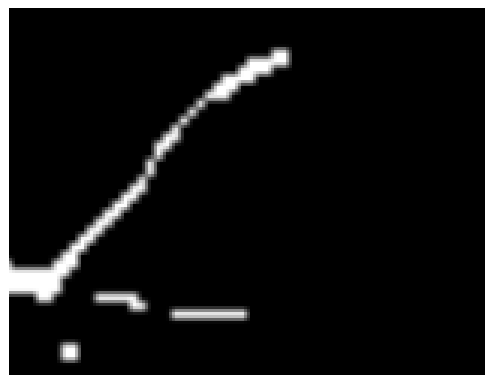


(d) Proposed model

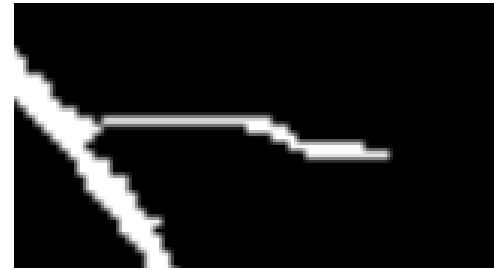
2D Results on DRIVE



(e) box 1



(f) box 2



(g) box 3

2D Result on DRIVE (details) top: standard TV ; bottom: directional TV



Our segmentation result compare favourably with the state of the art. Note that some learning-based approaches can still outperform these results.

	TP	TN	Acc
Standard TV	0.656	0.985	0.9421
Directional TV	0.690	0.981	0.9434
Staal [20]	-	-	0.9442
Human observer	-	-	0.9470

Quantitative segmentation results on the DRIVE database.



We have studied a thin object filtering methods called RORPO

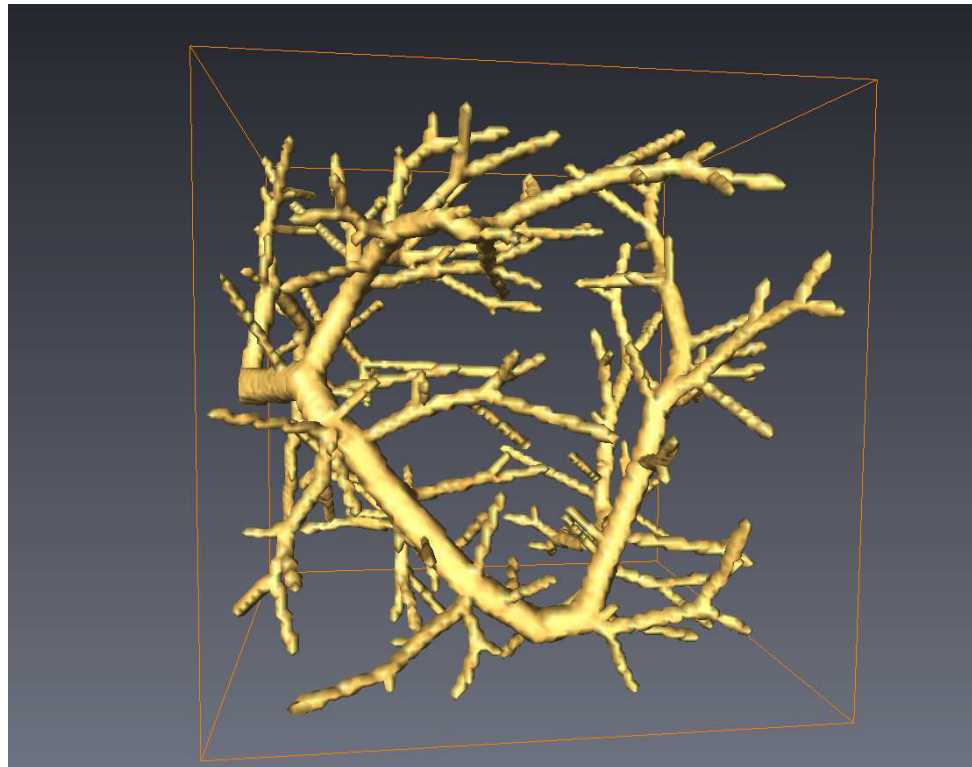
Associated with a multiscale approaches based on path length

Our method is effective at significantly reducing background noise while simultaneously suppressing non-tubular structures.



Quantitative evaluation of our results :

- Use phantoms produced by VascuSynth
- Use ground truth from heart MRA data.



- Produce images of scales
- Adapt the path operator framework to the max-tree/min-tree framework
 - This would allow discriminating objects on more complex measures than mere length
 - Think about incorporating robustness to max-trees / min-trees



- Definitions and early algorithms [2, 9, 10]
- Faster algorithms [1, 21]
- Extension to 3D and regularisation [12]
- RPO and 3D [5], [4]
- Applications [27, 28, 29, 19]
- RORPO [15, 16, 14]



References

- [1] Ben Appleton and Hugues Talbot. Efficient path openings and closings. In C. Ronse, L. Najman, and E. Decencière, editors, *Mathematical Morphology: 40 Years On*, volume 30 of *Computational Imaging and Vision*, pages 33--42, Dordrecht, 2005. Springer-Verlag.
- [2] M. Buckley and H. Talbot. Flexible linear openings and closings. In *Mathematical Morphology and its application to image analysis*, pages 109--118, Palo Alto, June 2000. Kluwer.
- [3] Tony F. Chan, Selim Esedoglu, and Mila Nikolova. Algorithms for finding global minimizers of image segmentation and denoising models. *SIAM J. Appl. Math.*, 66(5):1632--1648, 2006.
- [4] F. Cokelaer, H. Talbot, and J. Chanussot. Efficient robust d-dimensional path operators. *IEEE Journal of Selected Topics in Signal Processing*, 6(7):830--839, nov. 2012.



- [5] François Cokelaer. *Améliorations des ouvertures par chemins pour l'analyse d'images à N dimensions et implémentations optimisées*. PhD thesis, Université de Grenoble, 2013.
- [6] A. Dufour, O. Tankyevych, B. Naegel, H. Talbot, C. Ronse, J. Baruthio, P. Dokladal, and N. Passat. Filtering and segmentation of 3D angiographic data: Advances based on mathematical morphology. *Medical Image Analysis*, 17(2):147--164, 2013.
- [7] Alice Dufour, Christian Ronse, Joseph Baruthio, Olena Tankyevych, Hugues Talbot, and Nicolas Passat. Morphology-based cerebrovascular atlas. In *Biomedical Imaging (ISBI), 2013 IEEE 10th International Symposium on*, pages 1210--1214. IEEE, 2013.
- [8] A. Enquobahrie, L. Ibanez, E. Bullitt, and S. Aylward. Vessel enhancing diffusion filter. *ISC/NA-MIC Workshop on Open Science at MICCAI*, 7 2007.
- [9] H. Heijmans, M. Buckley, and H. Talbot. Path-based morphological openings. In *Proceedings of IEEE ICIP 2004*, pages 3085--3088, Singapore, October 2004.



- [10] H. Heijmans, M. Buckley, and H. Talbot. Path openings and closings. *Journal of Mathematical Imaging and Vision*, 22:107--119, 2005.
- [11] M. W. K. Law and A. C. S. Chung. Three dimensional curvilinear structure detection using optimally oriented flux. In *Proc. Eur. Conf. Comput. Vis.*, volume 5305 of *Lect. Notes Comput. Sci.*, pages 368--382. Springer, 2008.
- [12] C.L. Luengo Hendriks. Constrained and dimensionality-independent path openings. *Image Processing, IEEE Transactions on*, 19(6):1587--1595, 2010.
- [13] Adriënne M Mendrik, Evert-Jan Vonken, Annemarieke Rutten, Max A Viergever, and Bram van Ginneken. Noise reduction in computed tomography scans using 3-d anisotropic hybrid diffusion with continuous switch. *IEEE Trans. Med. Imag.*, 28(10):1585--1594, 2009.
- [14] Odyssée Merveille, Olivia Miraucourt, Stéphanie Salmon, Nicolas Passat, and Hugues Talbot. A variational model for thin structure segmentation based on a directional regularization. In *Image Processing (ICIP), 2016 IEEE International Conference on*, pages 4324--4328. IEEE, 2016.

- [15] Odyssee Merveille, Hugues Talbot, Laurent Najman, and Nicolas Passat. Tubular structure filtering by ranking orientation responses of path operators. In *Computer Vision--ECCV 2014*, pages 203--218. Springer, 2014.
- [16] Odyssée Merveille, Hugues Talbot, Laurent Najman, and Nicolas Passat. Ranking orientation responses of path operators: Motivations, choices and algorithmics. In *International Symposium on Mathematical Morphology and Its Applications to Signal and Image Processing*, pages 633--644. Springer, 2015.
- [17] Tuan-Anh Nguyen, Alice Dufour, Olena Tankyevych, Amir Nakib, Eric Petit, Hugues Talbot, and Nicolas Passat. Thin structure filtering framework with non-local means, gaussian derivatives and spatially-variant mathematical morphology. In *Image Processing (ICIP), 2013 20th IEEE International Conference on*, pages 1237--1241, Melbourne, Australia, September 2013.
- [18] Leonid I. Rudin, Stanley Osher, and Emad Fatemi. Nonlinear total variation based noise removal algorithms. *Phys. D*, 60(1-4):259--268, 1992.
- [19] Eysteinn Már Sigurðsson, Silvia Valero, Jon Atli Benediktsson, Jocelyn Chanussot, Hugues Talbot, and Einar Stefánsson. Automatic retinal



- vessel extraction based on directional mathematical morphology and fuzzy classification. *Pattern Recognition Letters*, 47:164--171, 2014.
- [20] Joes Staal, Michael D Abràmoff, Meindert Niemeijer, Max A Viergever, and Bram van Ginneken. Ridge-based vessel segmentation in color images of the retina. *Medical Imaging, IEEE Transactions on*, 23(4):501--509, 2004.
- [21] H. Talbot and B. Appleton. Efficient complete and incomplete paths openings and closings. *Image and Vision Computing*, 25(4):416--425, April 2007.
- [22] O. Tankyevych, H. Talbot, P. Dokladal, and N. Passat. Direction-adaptive grey-level morphology. application to 3d vascular brain imaging. In *Proceedings of ICIP 2009*, pages 2261--2264, Cairo, Egypt, 2009. IEEE.
- [23] O. Tankyevych, H. Talbot, P. Dokladal, and N. Passat. Spatially-variant morpho-hessian filter: efficient implementation and application. In *Mathematical Morphology and Its Application to Signal and Image Processing, Proceedings of the 9th International Symposium on Mathematical Morphology (ISMM) 2009*, pages 137--148, Groningen, The Netherlands, 2009.

- [24] O. Tankyevych, H. Talbot, N. Passat, M. Musacchio, and M. Lagneau. Angiographic image analysis. In G. Dougherty, editor, *Medical Image Processing: Techniques and Applications*, pages 115--145. Springer, 2011. ISBN 978-1441997692.
- [25] Olena Tankyevych. *Filtering of thin objects, applications to vascular image analysis*. PhD thesis, Université Paris-Est, October 2010.
- [26] Olena Tankyevych, Hugues Talbot, and Petr Dokládal. Curvilinear morpho-hessian filter. In *proceedings of the International Symposium on Biomedical Imaging (ISBI)*, pages 1011--1014, 2008.
- [27] S. Valero, J. Chanussot, J.A. Benediktsson, and H. Talbot. Détection automatique du réseau vasculaire rétinien basée sur la morphologie directionnelle et la fusion de décision. In *Proceedings of GRETSI*, Dijon, France, 2009. INIST-CNRS. Paru.



- [28] S. Valero, J. Chanussot, J.A. Benediktsson, H. Talbot, and B. Waske. Directional mathematical morphology for the detection of the road network in very high resolution remote sensing images. In *Proceedings of ICIP 2009*, pages 3725--3728, Cairo, Egypt, 2009.
- [29] S. Valero, J. Chanussot, J.A. Benediktsson, H. Talbot, and B. Waske. Advanced directional mathematical morphology for the detection of the road network in very high resolution images. *Pattern Recognition Letters*, 31(10):1120--1127, July 2010.